A Rock Magnetic Study of the Åkerberg Gold Deposit, Northern Sweden

Lars Dahlenborg

Examensarbeten i Geologi vid
Lunds universitet - Berggrundsgeologi, nr. 208

Geologiska institutionen
Centrum för GeoBiosfärsvetenskap
Lunds universitet
2007

A Rock Magnetic Study of the Åkerberg Gold Deposit, Northern Sweden

Master Thesis

Lars Dahlenborg

Department of Geology
Lund University
2007

Contents

Cover Picture: The open pit of the Åkerberg gold deposit, the photo was taken during the fieldwork 2006.

A Rock Magnetic Study of the Åkerberg Gold Deposit, Northern Sweden

Lars Dahlenborg

Dahlenborg, L., 2007: A Rock Magnetic Study of the Åkerberg Gold Deposit, Northern Sweden. *Examensarbeten i geologi vid Lunds universitet*, Nr. 208, 32 pp. 20 points.

Abstract: A rock magnetic study has been preformed of the Åkerberg gold deposit, located 30 km NE of Boliden in northern Sweden. The gold mineralization is located to a zone of subparallel quartz veins in a layered gabbro. Ground surveys show a lowering of the magnetic properties at the ore zone. This thesis addresses the factors causing the anomaly by investigating the magnetic properties of different parts of the gabbro. The thesis is also concerned with displacement of tectonic blocks, which is indicated by tilted magmatic layers in the immediate surroundings of the ore zone. Thermal and alternating field demagnetization and susceptibility and thermomagnetic measurements have been conducted on the samples collected at the ore zone and in distant parts relative to the ore zone. ChRM-directions have been analyzed with principal component analyses and one Virtual Geomagnetic Pole (VGP) was calculated. Mineral composition was examined with a Scanning Electron Microscope and conventional microscopy in both transmitted and reflected light. This study shows that the sampled outcrop distant to the ore zone is magnetite poor and that the gabbro lacks magnetite in the ore zone and in immediate surrounding areas. The NRM (Natural Remanent Magnetization) in the ore zone is carried by monoclinic pyrrhotite. The magnetic anomaly over the ore zone is caused by a lower amount of pyrrhotite compared to the surrounding areas. This study also indicates that the NRM carried by monoclinic pyrrhotite in the ore zone and in the distant parts of the gabbro was acquired during the same event. The timing of this event, however, is unclear since only one VGP could be calculated.

Keywords: NRM, gold ore, pyrrhotite, magnetite, Åkerberg.

Lars Dahlenborg, Department of Geology, GeoBiosphere Science Centre, Lund University, Sölvegatan 12, SE-223 62 Lund, Sweden. E-mail: l.dahlenborg@gmail.com

En bergartsmagnetisk studie av Åkerbergs guldgruva, norra Sverige

Lars Dahlenborg

Dahlenborg, L., 2007: En bergartsmagnetisk studie av Åkerbergs guldgruva, norra Sverige. *Examensarbeten i geologi vid Lunds universitet*, Nr. 208, 32 sid. 20 poäng.

Sammanfattning: En bergartsmagnetisk studie har utförts på en guldmineralisering som är belägen vid Åkerberg, 30 km Nordöst om Boliden, i norra Sverige. Mineraliseringen är bunden till en zon av subparallella kvartsgångar i en magmatiskt lagrad gabbro. Markbundna totalfältsmätningar av magnetismen visar en negativ anomali över malmzonen. I detta arbete har de magnetiska egenskaperna av området kring malmen, samt områden av gabbron som är mindre eller inte alls påverkade av malmlösningar undersökts. Arbetet syftar till att fastställa vad som orsakar anomalin. Detta arbete adresserar även tektoniska blockrörelser, vilket har observerats genom lutande lagring i närheten av malmzonen. Termisk- och växelströmsavmagnetisering har utförts på prover som inhämtats från malmzonen och mindre påverkade delar av gabbron. Utifrån dessa mätningar har olika vektorriktningar av NRM (Naturlig Remanent Magnetisering) analyserats och en så kallad VGP (Virtual Geomagnetic Pole) har beräknats. Ytterligare provundersökningar har varit susceptibilitet och termomagnetiska mätningar. Provernas mineralogiska sammansättning har undersökts med ett svepelektronmikroskop samt genom konventionell mikroskopering, så som i genomfallande och reflekterande ljus. Arbetet visar att magnetit som allmänt är ett av de vanligaste magnetiska mineralen, förekommer mycket sparsamt i de mindre påverkade delarna av gabbron (Fågelberget 1), samt att magnetit saknas i malmzonen och dess omgivning (Åkerberg 1 och Åkerberg 2). Det magnetiska mineralet i malmzonen är istället monoklin magnetkis. Den magnetiska anomalin är orsakad av en mindre mängd monoklin magnetkis i malmzonen jämfört med omgivande delar. Denna studie visar också att monoklin magnetkis i malmområdet, samt i mindre påverkade delar av gabbro, fick sin nuvarande NRM vid samma tidpunkt. Tidpunkten när detta hände har dock inte gått att fastställa då endast en VGP kunde beräknas.

Nyckelord: NRM, guldmalm, magnetkis, magnetit, Åkerberg.

Lars Dahlenborg, Geologiska Institutionen, Centrum för GeoBiosfärsvetenskap, Lunds Universitet, Sölvegatan 12, 223 62 Lund, Sverige. E-post: l.dahlenborg@gmail.com

1 Introduction

The ferrimagnetic minerals in a rock, such as magnetite and monoclinic pyrrhotite, can be ascribed to most magnetic anomalies in Precambrian terrains. The magnetic properties of these minerals reflect bulk rock composition, redox state, hydrothermal alteration and metamorphism. Rock magnetic studies, such as this thesis, address the magnetic minerals in a rock and can therefore be used to gain a better understanding of the magnetic signatures observed from surveys.

In this thesis, a magnetic anomaly observed at the Åkerberg gold deposit is investigated from a rock magnetic perspective. The gold deposit is situated 30 km northeast of Boliden, in the Västerbotten province of northern Sweden. The gold ore is located in a zone of subparallel quartz veins in a layered gabbro intrusive. During ground surveys conducted by Boliden Mineral AB, the gold bearing zone of Åkerberg showed a lowering of the magnetic properties. The main objective of this paper is to investigate this anomaly by comparing and quantifying the magnetic properties, such as the carriers of NRM (Natural Remanent Magnetization), Köningsberger ratios and susceptibilities, in different parts of the gabbro. At the end of this paper, a possible explanation of the magnetic anomaly is proposed.

Another aim of this paper is to investigate how different blocks may have moved relative to each other by analysing ChRM-directions (Characteristic component of Remanent Magnetization). Indications of block movements are found in the southern part of the open cut mine of Åkerberg, where the magmatic layers have been displaced. (This statement, however, assumes that the original magmatic layering was horizontal.)

The research in this paper is based on drill core samples collected during the summer 2006. To analyze the magnetic properties of the samples thermal- and alternating field demagnetization, thermomagnetic measurements and susceptibility measurements were conducted. Mineral composition was examined with Scanning Electron Microscope and conventional microscopy in both transmitted and reflected light

2 Geological Setting

2.1 The Skellefte District

The Skellefte district consists of volcanic, sedimentary and intrusive rocks, which occur in a NW-SE trending belt (Figure 1). To the south, the district borders a region of meta-sedimentary rocks with abundant granitoids. In the north, it passes into a region of less altered continental felsic volcanic rocks, intrusions and minor sediments.

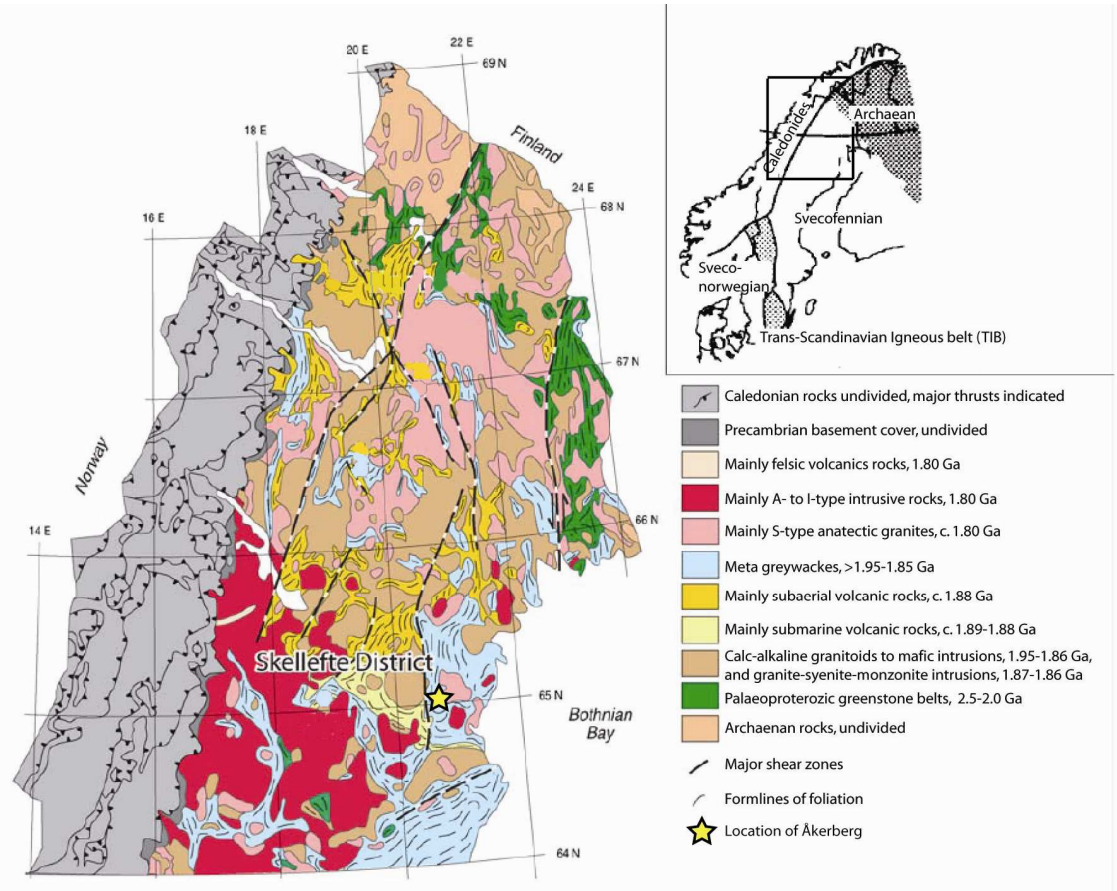

Figure 1. The figure shows the major bedrock units in northern Sweden. The Skellefte district is indicated by the light yellow submarine volcanic rocks in the lower center of the map. The figure has been modified after Weihed et al., 2005. The small map has been modified after Weihed, 1992.

The district is believed to have been formed in a volcanic arc environment during the Svecofennian orogeny, which took place 1.88-1.80 Ga (Lindström, 2000). The period was characterized by intense marine volcanism, that at different times and in different parts, changed into a period of reduced volcanism (Allen et al., 1997).

Complex horst and graben systems, isoclinal folds and shear zones dominate the structural geology in the area. The metamorphic conditions reached greenschist facies in the central parts of the district, but up to lower amphibolite facies in the south, western and eastern parts (Allen et al., 1997).

The volcanic and sedimentary rocks of the Skellefte district are divided into different groups. The lowest stratigraphical unit is the Skellefte group. Volcanoclastic rocks, porphyritic intrusions and lavas dominate the _group, but sedimentary rocks, such as mudstone, volcanoclastic siltstone, sandstone and breccia conglomerates are also included (Allen et al., 1997). U-Pb dating of the stratigraphical upper parts of the Skellefte group suggests an age of 1882 ± 2 Ma (Welin, 1987).

The Vargfors group, which overlays the Skellefte group, consists of fine- to coarse-grained sedimentary successions. Ages and stratigraphical relationships suggest that the Vargfors group is up to 10 Ma younger than the Skellefte group (Allen et al., 1997).

The Arvidsjaur group, which is of similar age to the Vargfors group, is interpreted as a lateral equivalent to the Vargfors group. Subaerial and intermediate volcanic rocks are characteristic for this group (Allen et al., 1997).

The volcanic and sedimentary rocks of the Skellefte district are intruded by syn- and post depositional mafic- to felsic intrusions. The intrusions are divided into different suites according to their time relationship to the Svecofennian orogeny. The oldest suite consists of the Jörn granitoids. The Jörn suite ranges in composition from gabbro to granite. Several features, such as composition, radiometric ages and intrusive contacts, suggest that the Jörn suite may be comagmatic with the Skellefte and Arvidsjaur volcanism (Allen et al., 1997).

The Skellefte-Härnö suite is composed of late to post Svecokarelian granites. The suite lacks mafic members and is believed to have originated from partial melting of sedimentary rocks. The Skellefte-Härnö suite is divided into two types. One type is heterogeneous and the other type is homogenous and has a more intrusive character. The ages of Skellefte-Härnö are between 1809 ± 8 Ma and 1798 ± 2 Ma. (Kathol & Weihed, 2005).

The rocks of the Revsund suite are interpreted to be a part of the TransScandinavian Igneous Belt (TIB) (Kathol & Weihed, 2005). The suite intruded during the final phase of the Svecokarelian orogeny and lacks the tectonic structures of deformation, which can be seen in the early suites. The ages of these rocks show an overlap with the Skellefte-Härnö suite (Kathol & Weihed, 2005).

Economically, the Skellefte district is one of most important ore regions in Sweden. A large number of mineralizations, deposits and ores are in the area. The most common type is volcanogenic massive sulfide deposits (VMS). The Skellefte group hosts most of these VMS. Gold has been mined as a byproduct ever since the well-known Boliden gold mine ceased production in 1967 (Sundblad, 2003). It was not until the late 1980s, with the discovery of the Björkdal and Åkerberg gold deposits, that the Skellefte district could also be regarded as a lode gold district.

2.2 Local Geology

Figure 2 shows the bedrock in the Åkerberg area. To the east meta-sediments (indicated by the color blue on the map) dominate the bedrock. The contact between the meta-sediments and the meta-gabbro is of both intrusive and tectonic character.

The meta-gabbro (indicated by the color green in Figure 2) is the host rock for the gold mineralization in the Åkerberg deposit. The meta-gabbro is characterized by a diffuse magmatic layering, which is often distinguished by parallel orientation of plagioclase or variations in mineralogical composition (Mattsson, 1991). Its age has been determined with the mineral baddelyite. Preliminary results show an age of 1878 ± 2Ma (pers. comm. Ulf Söderlund, 2006).

The meta-gabbro is intruded by a fine grained meta-granodiorite (indicated by the color brown in Figure 2) with an age of 1880-1870 Ma (Bergman Weihed, 1997). Horizontal sheets of pegmatite are common in the area and one lithium pegmatite is well exposed in the open cut mine of Åkerberg.

The bedrock surrounding the gabbroic intrusion is dominated by Skellefte type granite (indicated by the color orange in Figure 2) and minor occurrences of Revsund type granites.

The time relationship of the different intrusive rocks and the meta-sediments can be summarized as (from oldest to youngest): meta-sediment, meta-gabbro, granodiorite and Skellefte type granite and pegmatite dyke and, finally, Revsund type granite. The gold mineralization is cut by the granodiorite and is therefore interpreted as older than the granodiorite.

Many shear and deformation zones with different orientations have been observed in the Åkerberg area and it can be described as structurally complex.

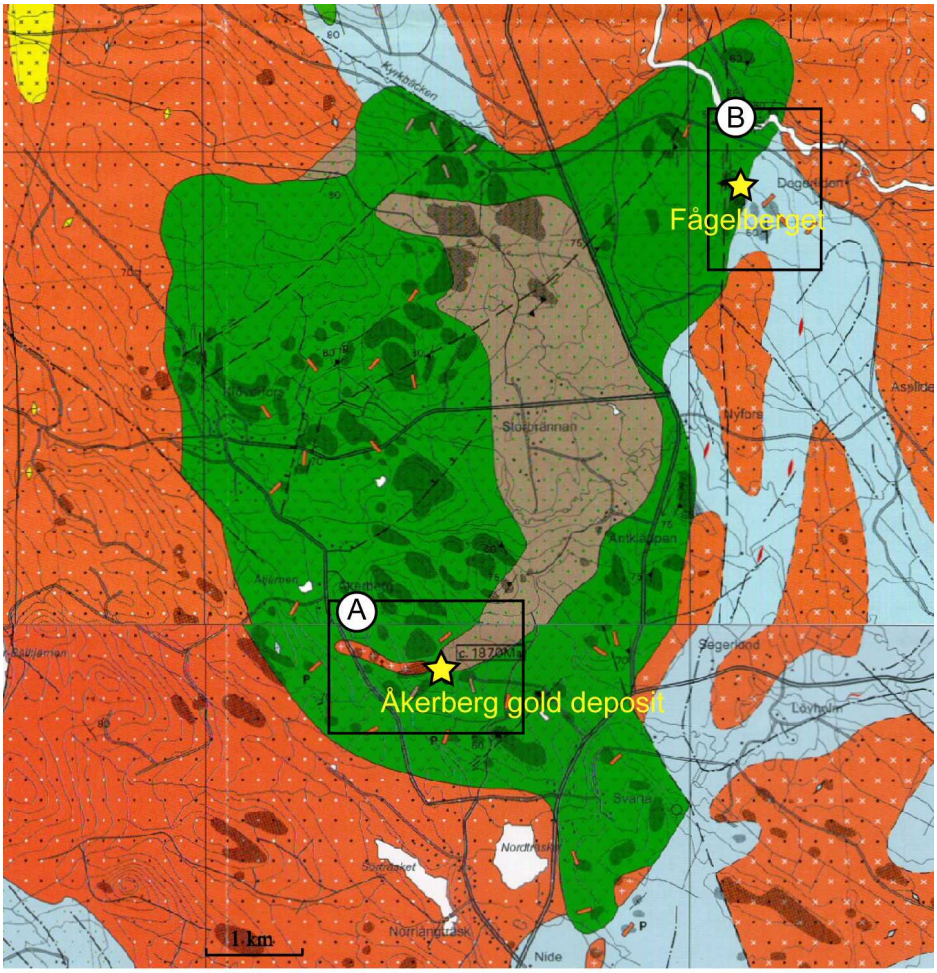

Figure 2. The map shows the meta-gabbro and location of the sampled outcrops. At Åkerberg gold deposit two outcrops were sampled, the scale of the map however, makes it impossible to separate them. The marked areas A and B shows the areas of the magnetic anomaly maps in Figure 7. From map sheet Boliden 23K SO and Boliden 23K NO (Sveriges Geologiska Undersökning, premission: 30-265/2007)

2.2.1 The Gold Mineralization in Åkerberg

The ore zone has an E-W orientation. Before the gold ore was mined, the ore zone was c. 10 m wide and characterized by millimeter wide quartz veins, which could be as abundant as >100 per every 2 m. Occasionally, the ore zone could be up to 30 m wide due to overlapping from shearing in the ore zone (pers. comm. Benny Mattsson, 2006).

The length of the mineralization was 350 m and could be followed to a depth of 150 m in the western part. In the eastern part, it is intruded by the granodiorite. When mined, the ore had a gold content of 3 g per metric ton (Mattsson, 1991).

The gabbro is structurally complex and the kinematic evolution in the area is largely unknown. Dextral movement has been recorded in the horizontal plane of the ore zone, and morphology of structures suggest an upward movement of the northern parts relative the southern parts (pers. comm. Benny Mattsson, 2006).

3 Fieldwork

The fieldwork was carried out during the end of August 2006. It aimed to localize and sample outcrops that were suitable to the objectives of the thesis. For rock sampling, a handheld diamond drill (also referred to as a paleomagnetic drill) was used. The drill crown had an inner diameter of 2.57 cm.

Each drill core was orientated with sun and magnetic compasses before being removed from the outcrop. The length of each collected core was between 6 and 8 cm and thirty drill cores were collected.

The local magnetic declination in the area at the time of sampling was ~6° (National Geophysical Data Center, 2006) (sampling date: end of August and mid September 2006).

4 Laboratory Procedures and Rock Magnetic Background

4.1 A Brief Introduction to Rock Magnetism.

In this section some aspects of rock magnetism, which are general but not related to the laboratory procedures in this thesis, will be mentioned. If not otherwise stated, the background information in this and the following sections in Chapter 4 are referred to Robert Butler's excellent book, Paleomagnetism (Butler, 1991).

A major goal of rock magnetic studies is to understand the origins and properties of remanent magnetization (RM). RM is defined as magnetization that exists in the absence of an external magnetic field. The remanent magnetization of a rock sample prior to laboratory treatment is called Natural Remanent Magnetization (NRM). NRM depends on the geomagnetic field and geological factors during the formation of the rock. When NRM is studied, it is subdivided into primary and secondary NRM. In ideal conditions, primary NRM is the magnetic component acquired during rock formation and the secondary NRM is acquired subsequent to rock formation.

In a rock, ferrimagnetic minerals carry NRM. The most important of these minerals are iron-titanium oxides, such as titanomagnetites, and, in some cases, iron sulfides, such as pyrrhotite. Beside the ferrimagnetic minerals, there are also paramagnetic minerals in a rock. These minerals consist of iron-silicates, such as amphibole and pyroxenes. Paramagnetic minerals do not contribute to the NRM of a rock.

An important topic in rock magnetism is grain size. Ferrimagnetic grains can be described as single domain (SD), multi domain (MD) or pseudo-single-domain (PSD). A domain is a volume in the grain where the quantum mechanic spins of electrons are aligned which in turn creates a magnetic field. SD grains are so small that they only have one magnetic domain. The critical size of the SD-grains varies between different minerals. For magnetite, the critical size is c. 0.06 :m (depending on grain shape) and for pyrrhotite, it is c. 1.6 :m (Dunlop & Özdemir, 2001). MD grains have several magnetic domains. The total sum of the magnetic domain moments constitutes the total magnetic moment of the grain. PSD-grains exist between grain sizes of very small MD-grains (with only a few domains) and large SD-grains.

There are some important differences between these types of grains. SD-grains have higher coercivities than MD- and PSD-grains. (Coercivity is a magnetic property of a material's ability to resist an external magnetic field, high coercivity means high resistance). SD-grains are also more efficient carriers of remanent magnetization compared to MD- and PSD-grains.

Ferrimagnetic minerals also have the ability to record applied magnetic fields, such as the geomagnetic field. The ability to record this is largely temperature dependent, but the meaningful information is that ferrimagnetic minerals can preserve paleogeomagnetic fields and carry this information over geologically significant time. If a paleopole is successfully determined, it can reveal information such as timing of NRM acquisition, which is obtained by comparing the calculated paleopoles to paleopoles from rock units that have been dated.

4.2 Demagnetization Techniques

The objective of the demagnetization procedures is to successively break down the NRM, which is carried by ferrimagnetic minerals in the samples. There are different methods of doing this. In this paper, alternating field (AF-) and thermal demagnetization were used.

During both thermal and AF-demagnetization, susceptibility is measured along the X-, Y- and Z-axes of the sample at each demagnetization level. The NRM-vectors at different demagnetization levels are then recorded. The data is fundamental during the calculation of paleomagnetic poles, which is described in section 4.2.1.

The results of AF- and thermal demagnetization are illustrated in diagrams where the Y-axis represents normalized remanence, and the X-axis represents different levels of alternating fields or thermal demagnetization temperatures. Depending on the shape of the curves these diagrams can indicate the ferrimagnetic minerals in a sample. However, other investigations are also necessary to determine the ferrimagnetic minerals in a sample.

The differences between AF-demagnetization and thermal demagnetization will now be explained. During AF-demagnetization, a sample is exposed to an alternating magnetic field. At low levels, the ferrimagnetic grains with low coercivity are then erased. (Coercivity is the magnetic property of a material's ability to resist an external magnetic field, (i.e.) high coercivity means high resistance). The alternating magnetic field is successively increased during the demagnetization, and ferrimagnetic grains with suc-

cessively higher coercivities are then erased. When there is no secondary alteration of minerals, low coercivity grains are likely to carry secondary NRM (NRM induced after rock formation) and AF-demagnetization thus leaves the sought primary NRM, (NRM acquired during rock formation) unaffected.

Like AF-demagnetization, the objective of thermal demagnetization is to successively break down the NRM carried by ferrimagnetic minerals. The NRM is erased when the demagnetization temperature exceeds the blocking temperature for the ferrimagnetic mineral. The blocking temperature (T_b) is related to the Curie Temperature (T_C) but the T_b is always lower than the T_C.

Ferrimagnetic minerals have different T_C, which are each characteristic for those minerals. The shape of the thermal demagnetization curves can therefore indicate the ferrimagnetic phases in the sample. Some ferrimagnetic minerals such as titanomagnetites, titanohematites or pyrrhotite can have similar blocking temperatures (depending on mineral composition and grain size). When such phases are suspected, additional investigations and measurements are required.

4.2.1 Analyses and Presentation of Demagnetization Data

In the previous chapter (Chapter 4.2), it was mentioned that the directions of the NRM-intensities were measured during different demagnetization steps along the X-, Y- and Z-axes of a sample. During demagnetization the ferrimagnetic grains with low T_b or coercivity are broken down first. If these low T_b or low coercivity grains carry different NRM-directions (which could be due to thermal or viscous overprinting) than the grains with high T_b or coercivity, the recorded NRM-directions along the X-, Y- and Z-axes will change at higher demagnetization levels. Therefore, to make sure that the obtained NRM-directions are characteristic for the sample, the NRM-directions must be analyzed. In this thesis, the NRM-directions were analyzed with the computer program SUPER-IAPD (Geodynamics, 2006). These analyses are done in three different steps, which will now be explained.

The data is first plotted in a Zijderveld diagram, which a 2-dimensional way to present the 3-dimensional NRM-vectors measured along the samples X-, Y- and Z-axis during different Thermal and AF-demagnetization steps. An example of a Zijderveld diagram is shown in Figure 3. Each NRM-vector in a Zijderveld diagram is labeled with a number corresponding to the demagnetization level. Point 0 °C indicates NRM prior to demagnetization. The solid boxes represent vector end-points plotted on a horizontal plane. The open boxes represent vector end-points plotted on a vertical plane.

In certain intervals, the Zijderveld diagrams have linear segments whose directions are related to the declination and inclination of the resolved components (e.g. NRM-direction). Such a segment is also marked in Figure 3.

The identified component(s) in a sample is inspected visually with the computer program Super-IAPD in order to determine declination/inclination (decl/incl). The objective of this analysis is to identify the component(s) that can be regarded as the characteristic component(s) of the sample. This component(s) is generally called characteristic component of remanent magnetization (ChRM).

It is sometimes possible to identify more than one component in a sample. Some samples can also show evidence of overlapping blocking temperatures or coercivity spectra. In such cases, more than one coercivity or blocking temperature is present within the same demagnetization interval. In Zijderveld diagrams, the plotted vectors are then displayed as curves instead of straight lines and no data can be obtained from them. Examples of two NRM-directions and overlapping blocking temperatures (or coercivity) from samples analyzed in this paper are given in Figure 10 (Chapter 7-Results).

Identified ChRM-directions are presented as lines in a stereogram. In the stereogram it is possible to determine how different directions relate to each other, e.g. if they scatter or group. The vectors plotted in a stereogram are also used to calculated paleopoles. This is done with a method developed by Fisher in the 1950s and is generally referred to as the Fisher distribution. Fisher distribution yields several statistical parameters for the plotted ChRM-directions, which makes it possible to group vectors with similar directions. The mean direction of each group is used to calculate the paleopoles. For statistical reasons several groups with similar directions are required when a paleopoles is determined. If only one or a few groups are used, the calculated poles are referred to as Virtual Geomagnetic Poles (VGPs).

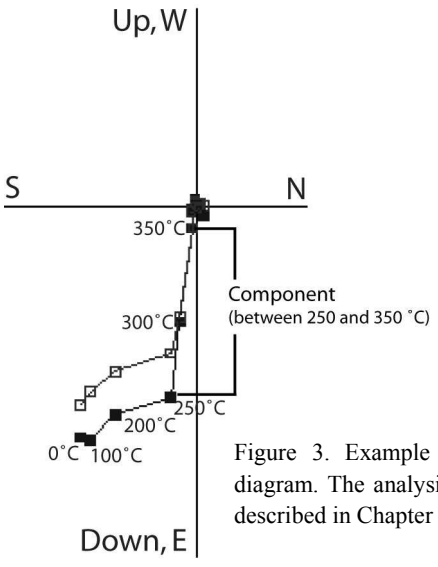

Figure 3. Example of Zijderveld diagram. The analysis procedure is described in Chapter 4.2.1.

4.2.2 Demagnetization Measurement Data

Demagnetization was carried out in the paleomagnetic laboratory at Lund University with a 2G-SQUID rock magnetometer. AF-demagnetization was made in intervals between 0-10 mT in steps of 2 mT (Tesla), and between 10-50 mT in steps of 5 mT. At alternating fields higher than 50 mT steps of 10, 20 or 25 mT were used. Demagnetization continued until all substantial remanence was erased or became unstable. The maximum fields applied were 100-150 mT.

Thermal demagnetization was conducted with a MMTD80 oven. Samples were heated to 100, 200, 250, 300, 350, 400, 500, 540, 560, 580, and 600 °C. The magnetization was measured at each step starting at room temperature with the equipment mentioned above.

4.3 Susceptibility Measurements

The susceptibility of the samples was measured with a KLY-2 susceptibility bridge from Geophysica Brno.

Susceptibility is a material's ability to become magnetized. In a geological context, susceptibility is a mineral's ability to become magnetized. During susceptibility measurements, an external magnetic field is applied to the sample and a new internal field is then created. This phenomenon is called induced magnetism and occurs in all minerals. Susceptibility measurements are important as they indicate different kinds of magnetic behaviors, such as dia-, para-, and ferrimagnetism. Diamagnetism results in negative susceptibilities because the internal magnetic field, created during induced magnetism, is opposite the external magnetic field. Para- and ferrimagnetism results in positive susceptibilities because the internal magnetic field, created during induced magnetism, is aligned with the external magnetic field.

The magnetic behaviors dia-, para-, and ferrimagnetism are characteristic for the minerals in a sample. For example, silicates such as iron rich amphiboles and pyroxenes show a paramagnetic behavior, whereas iron oxides or iron sulfides such as magnetite and monoclinic pyrrhotite show ferrimagnetic behavior.

Susceptibility measurements are useful as they can be used to assess the concentrations of ferrimagnetic minerals in a sample (Peters & Dekkers, 2003). This observation is important and will be used later in this thesis.

4.4 Calculation of Köningsberger Ratios

The susceptibility data and the NRM-intensities obtained from demagnetization were used to calculate the Köningsberger ratios (Q). Q is the quotient of the remanent magnetization and the field induced in the rock by the geomagnetic field (Q= (NMR)/χH. Where χ = susceptibility and H = geomagnetic field). Ratios of Q >1 are considered good since they indicate that the magnetism has not been overprinted or acquired viscous overprint. Typical Q-values for a gabbro range from 1-9.5 (Hunt et al., 1995). These values may be different for magnetite and pyrrhotite bearing rocks.

4.5 Determination of Ferrimagnetic Minerals with Thermomagnetic Curves

During thermomagnetic measurements, the susceptibility is measured as a function of temperature. The susceptibility in the mineral changes during increased temperature, and when it reaches the blocking temperature of a mineral it disappears. The results are displayed as curves in a diagram. The normalized susceptibilities of the samples are plotted against the temperatures during a heating and a cooling phase. The behavior of the thermomagnetic curves are often described as reversible or irreversible. Reversible means that both the heating and cooling phase coincide, whereas irreversible means that the heating and cooling phase are different. Thermomagnetic curves can also reveal mineral properties such as Curie temperatures (T_C) or Néel Temperature (T_N) for a mineral. If the T_C/T_N can be determined for a thermomagnetic curve, it is a very good indicator of the ferrimagnetic phase in the sample.

4.5.1 Thermomagnetic Measurement Data

Five samples were selected for measurements due to different thermal and AF-demagnetization curves. The apparatus used was a CS-3 Temperature Control Unit connected to a KLY-2 susceptibility bridge. A small part of each sample was ground to a sand sized fraction. Each grounded sample was then placed in a test tube. Measurements started at room temperature and ended at 420 °C or 610 °C, and then they were cooled to 50 °C. Susceptibility was measured continuously during both the heating and cooling phases.

4.6 Optical and SEM-investigations

Fourteen samples were selected for optical investigations. The selection was made so that a thin section should be representative for each site regarding demagnetization curves, susceptibility and where the sample was taken (e.g. magmatic layering). When a site lacked continuity in the mentioned parameters, more than one sample were selected.

The thin sections were 30 µm thick. Examination was made in reflective and plane polarized light to identify opaque and transmitting mineralogy, respectively.

From each site, samples were selected for Scanning Electron Microscopy (SEM). They were selected to ensure correct interpretations of opaque phases and to identify fractions and grain sizes too small for conventional microscopy. Since the sites from Fågelberget yielded more incoherent demagnetization results, more emphasis was put on these during SEM-investigations.

5 Description of the Sampled Sites

Three outcrops were selected for sampling. The selection was done so the outcrops would be representative for the mine area and parts less or not affected by ore bearing fluids. It was also important that the magmatic layering was visible, as this was fundamental when investigating block movement. The block movement is indicated by displaced magmatic layers. The rotation, however, in this movement is not visible.

In the three selected outcrops, different sites were placed. A site is a paleomagnetic term for a sampled locality. For statistical reasons one site consists of five or more drill cores. Therefore, when more than five samples are placed in an outcrop the additional samples are regarded as another site.

A description of the outcrops, and how they were sampled, is provided below. The abbreviated names in this section will be used later in the paper. The different outcrops are also summarized in Table 1.

Table 1.

Outcrop	Name	Number of samples
Åkerberg 1	Åke 1	5, a-e
Åkerberg 2	Åke 2	10, a-e, and f-j
Fågelberget 1	Fåg 1	15, a-e, f-j and k-o

Table 1. Outcrop names and abbreviated site names. From each site five samples were taken, a-e, f-j and k-o denotes individual samples.

Åkerberg 1 (Åke 1, samples a-e)

This outcrop was sampled so the magnetic properties of the ore zone could be investigated. The outcrop is situated in the prolongation of the main gold bearing zone of Åkerberg, in the western part of the open cut mine. The main zone is a part of a shear zone that cuts the gabbro with an E-W orientation. It is characterized by quartz filled joints (width <1cm) with the same orientation as the main shear zone (Figure 4).

The sampled outcrop was located in the floor of the open pit. There was no visible magmatic layering in this outcrop. Therefore observations from Åke 2 (next section), where the magmatic layering was visible, were implemented when drilling. Five samples were taken from this outcrop, they are referred to as Åke 1 (sample names a-e).

Åkerberg 2 (Åke 2 a-e and Åke 2 f-j)

This outcrop was sampled so the magnetic properties close to the ore zone could be analysed. It represents the non anomalous area surrounding the ore zone and shows displaced magmatic layers. The outcrop is situated just outside the mineralized area.

In the lower parts of the outcrop a magmatic lay-

Figure 4. The photo is from the Åkerberg open cut mine. Note the vertical quartz veins, which are characteristic for the gold mineralization in the ore zone.

Figure 5. Photo of the magmatic layering observed in the second outcrop sampled at Åkerberg. See section Åkerberg 2 for a description of the outcrop.

ering is clearly visible, but only at the weathered surface and not in a fresh cut surface (Figure 5). The strike and dip of the layers is to N160/75°. In the middle part of the outcrop, no magmatic layers are visible, which could be due to the thickness of the layer or to minor compositional variations of the layers. In the upper most part of the outcrop fine grained fragments of unknown origin appear. Drilling was avoided at these parts.

Ten samples were taken in Åke 2 (sample names a-e and f-j), five in the middle part and five in the lower part.

Fågelberget 1 (Fåg 1a-e, Fåg 1f-j and Fåg 1k-o)

This outcrop was sampled as it is situated far away from the magnetic anomaly of the ore zone. It shows a clear magmatic layering and is unaffected by ore bearing fluids (Bolidens analysis, pers. comm. Jakob Fahlgren and Benny Mattsson).

The Fågelberget outcrop is situated 6 km northeast of the Åkerberg gold deposit, close to a regional shear zone, which separates the meta-gabbro from meta-sediments (Figure 2). Generally the meta-sediments are found tectonically incorporated in the meta-gabbro at the contact. No incorporated sediments were, however, observed in the outcrop of Fågelberget.

The magmatic layering of this outcrop is very close to being horizontal and the layers are clearly visible. Three layers were recognized in the outcrop (Figure 6). The visible bottom layer had a fine to medium grain size and on the weathered surfaces it appeared to be rich in feldspars. Overlaying this layer there was a coarse grained layer, which was rich in amphibole. The visible top layer, which also constituted the top of the outcrop, had a fine to medium grain size and it appeared to be rich in feldspars (similar to the bottom layer). The contact between the bottom and middle layer was sharp.

Fifteen samples were taken in Fåg 1 to assess the magnetic properties of the layers. Five samples in the bottom (Fåg 1a-e), more feldspar rich layer, five in the middle layer (Fåg 1f-j), which were more amphibole rich, and finally five in the contact between the layers (Fåg 1k-o).

Figure 6. Photo of the magmatic layering observed in Fågelberget. See section Fågelberget 1 for a description of the outcrop

6 Local Geophysics

Boliden Mineral AB has conducted all ground geophysical surveys in the area and has also supplied the material in this paper.

The magnetic anomaly map shows the area over the sampled localities, Åkerberg gold deposit (Figure 7a) and Fågelberget (Figure 7b). The magnetic survey was preformed before the mining started. Measurements were conducted in a grid of 20x20 m outside the ore zone and in a grid of 10x10 m over the ore zone. The color scale of the map follows the same relative principle as a topographic map. Blue color indicates lower field values, green indicates higher values and brown even higher (peak values are indicated by the color gray).

When interpreting the magnetic map, the meta-gabbro is easily distinguished from other rock units due to higher field values (green to brown color). Fågelberget (7b) is located in the margin of the meta-gabbro. This area of the meta-gabbro shows higher magnetic field values relative to other parts of the meta-gabbro. The increase is interpreted as due to abundant iron oxides.

The area over the open pit (7a) shows a lowering of field magnetic values, similar to those of the granodiorite. This is an important observation as there are many shear zones in the meta-gabbro, but very few that causes such an obvious decrease in magnetism which have been recorded in the ore zone of Åkerberg.

Gravimetric surveys have also been conducted and they indicate that the meta-gabbro is a rather thin body (Lundström & Antal, 2000).

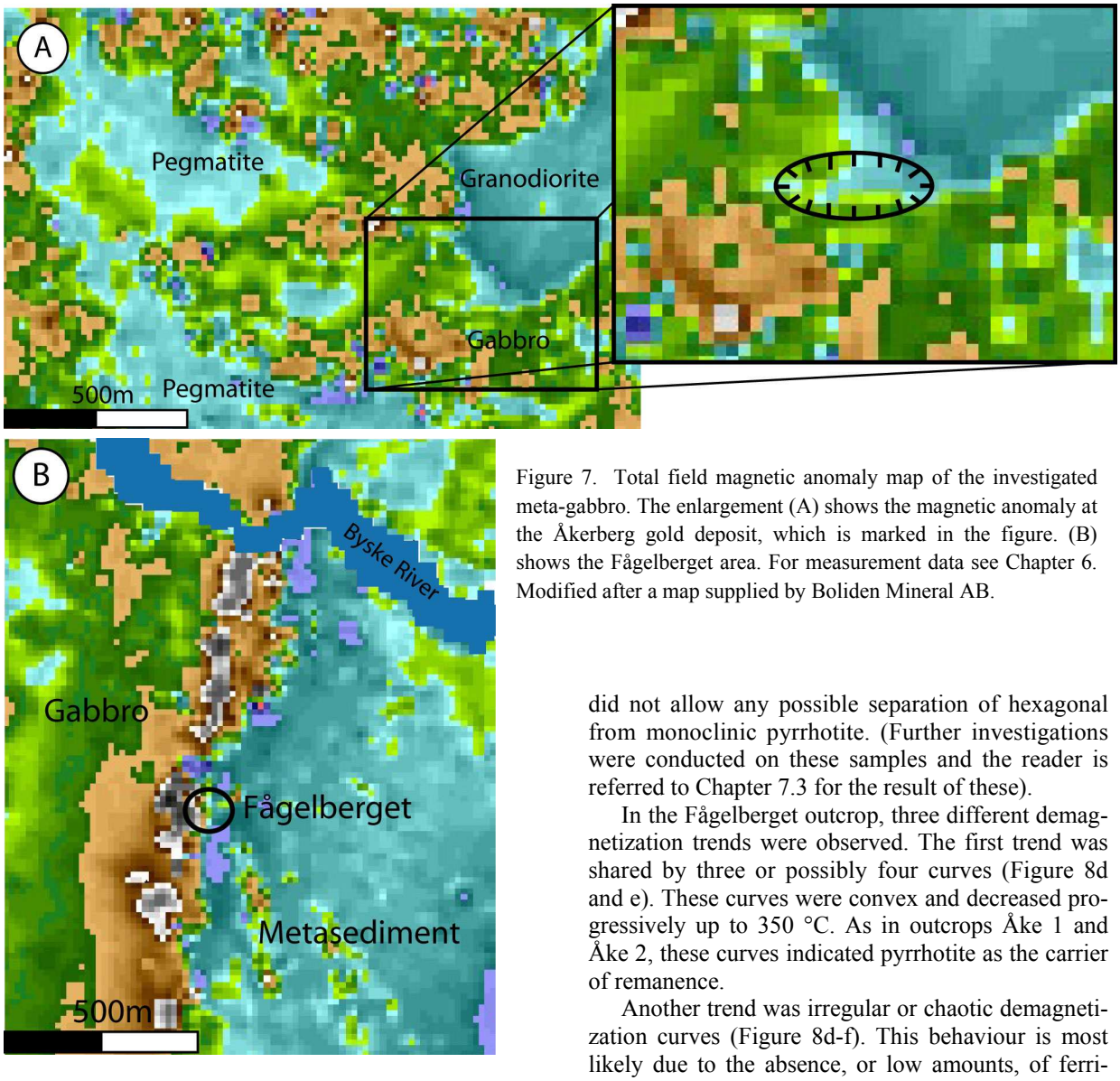

Figure 7. Total field magnetic anomaly map of the investigated meta-gabbro. The enlargement (A) shows the magnetic anomaly at the Åkerberg gold deposit, which is marked in the figure. (B) shows the Fågelberget area. For measurement data see Chapter 6. Modified after a map supplied by Boliden Mineral AB.

7 Results

7.1 Demagnetization Results

7.1.1 Thermal Demagnetization Results

The following text describes the different observed thermal demagnetization behaviors. All demagnetization curves discussed in this section are shown in Figure 8.

The two outcrops Åke 1 and Åke 2 showed almost identical demagnetization trends (Figure 8a-c). The curves were convex (the use of *convex* in this thesis referrers to convex downwards) and decreased progressively up to temperatures of 350 °C without much noise. The curves thus indicated pyrrhotite (T_N=310-325 °C) as the carrier of remanence (Dekkers, 1989). Thermal demagnetization, however, did not allow any possible separation of hexagonal from monoclinic pyrrhotite. (Further investigations were conducted on these samples and the reader is referred to Chapter 7.3 for the result of these).

In the Fågelberget outcrop, three different demagnetization trends were observed. The first trend was shared by three or possibly four curves (Figure 8d and e). These curves were convex and decreased progressively up to 350 °C. As in outcrops Åke 1 and Åke 2, these curves indicated pyrrhotite as the carrier of remanence.

Another trend was irregular or chaotic demagnetization curves (Figure 8d-f). This behaviour is most likely due to the absence, or low amounts, of ferrimagnetic phases in the samples. Some of the samples that showed a strong increase in magnetization between demagnetization temperatures of 540-580 °C (Figure 8e). This increase can be attributed to mineralogical reactions in the samples.

Some samples also showed demagnetization trends that were more stable (Figure 8f). The demagnetization curves of these samples decreased progressively up to temperatures of 560-580 °C. The other curve showed a small increase up to 250 °C and then started to decrease to reach a minimum at 540-580 °C (Figure 8f).

The ChRM-direction from the Åke 1 and Åke 2 outcrops are shown in Figure 10 a-c. These directions had a T_b of 250-350 °C. When plotted in Zijderveld diagrams these samples often showed two directions. In such cases, the direction corresponding to a higher T_b was selected. An example of a Zijderveld diagram with two NRM-directions is shown in Figure 11a.

ChRM-directions from the Fågelberget outcrop showed positive and negative inclination (Figure

10d-f). The directions with positive inclination had a T_b of 250-350 °C (Figure 10d), whereas the directions with negative inclination generally showed a higher T_b (Figure 10f).

From samples in the Fåg 1 outcrop, which showed irregular demagnetization trends little or no ChRM-directions were obtained. When plotted in a Zijderveld diagram it was common that they were irregular. From samples showing this behaviour, little or no paleomagnetic data was obtained.

7.1.2 Alternating Field Demagnetization Results

The following text describes the different observed AF-demagnetization behaviors. All demagnetization curves discussed in this section are shown in Figure 9.

The demagnetization curves of Åke 1 showed rapidly decreasing intensities up to 8 mT (Tesla) (Figure 9a). At higher fields the curves were more irregular. The Åke 2 outcrop showed rapidly decreasing intensities up to 10mT for all samples (Figure 9b-c). The slopes of the curves from this outcrop and the Åke 1 outcrop were the same, which indicated that the carrier of remanence in these samples had a similar coercivity.

In the Fågelberget outcrop, four samples showed a demagnetization trend that decreased rapidly up to 10 mT (Figure 9d-e). These curves were similar when compared to the demagnetization curves observed for outcrops Åke 1 and Åke 2.

Some samples from the Fågelberget outcrop were

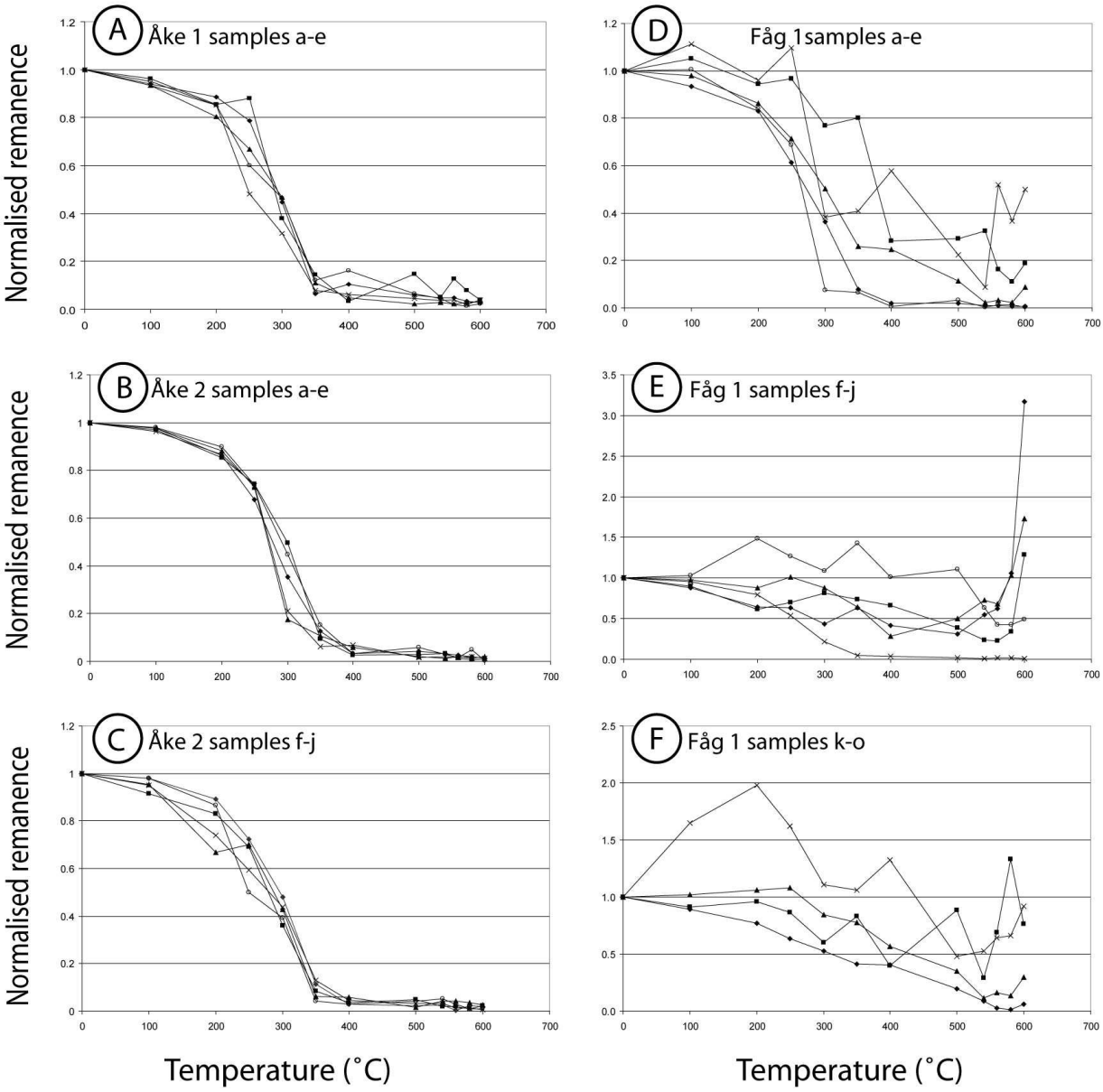

Figure 8. Thermal demagnetization curves for the investigated outcrops. The curves have been normalized with their initial intensities (J_s/J_0). 8f differs as it only has four demagnetization curves, which is due to a computer error during measurement. **NOTE DIFFERENT SCALE ON Y- and X- AXES.**

more irregular during AF-demagnetization (Figure 9d-f). This behaviour can be attributed to a low amount of ferrimagnetic phases in the samples.

In Fågelberget, some samples also showed evidence of a higher stability component. These demagnetization curves decrease successively up to 80-100 mT (Figure 9e) or up to 30 mT (Figure 9f).

The ChRM-directions in outcrops Åke 1 and Åke 2 are shown in Figure 10 a-c as solid circles, which indicate positive inclination. Most of these directions were stable in an interval of 2-10 mT (the stability for individual samples are show in Figure 10). Some samples, especially from outcrop Åke 1 showed overlapping coercivity spectras, and an example of this is shown in Figure 11b. It was not possible to separate the different components from samples that behaved this way, and no palaeomagnetic data was obtained from the samples.

Samples from Fågelberget outcrop showing a similar demagnetization trend compared to Åke 1 and Åke 2 gave similar ChRM-directions with similar stability, which can be seen in Figure 10d.

From samples that yielded irregular demagnetization curves, which were observed in Fågelberget, also yielded irregular Zijderveld diagrams. An example of this is shown in Figure 11c. These samples did not yield any ChRM-directions.

The curves from Fågelberget that showed evidence of a higher stability component yielded ChRM-directions with negative inclinations (open circles in Figure 10e-f). These directions were generally stable in higher alternating fields, up to 15 mT.

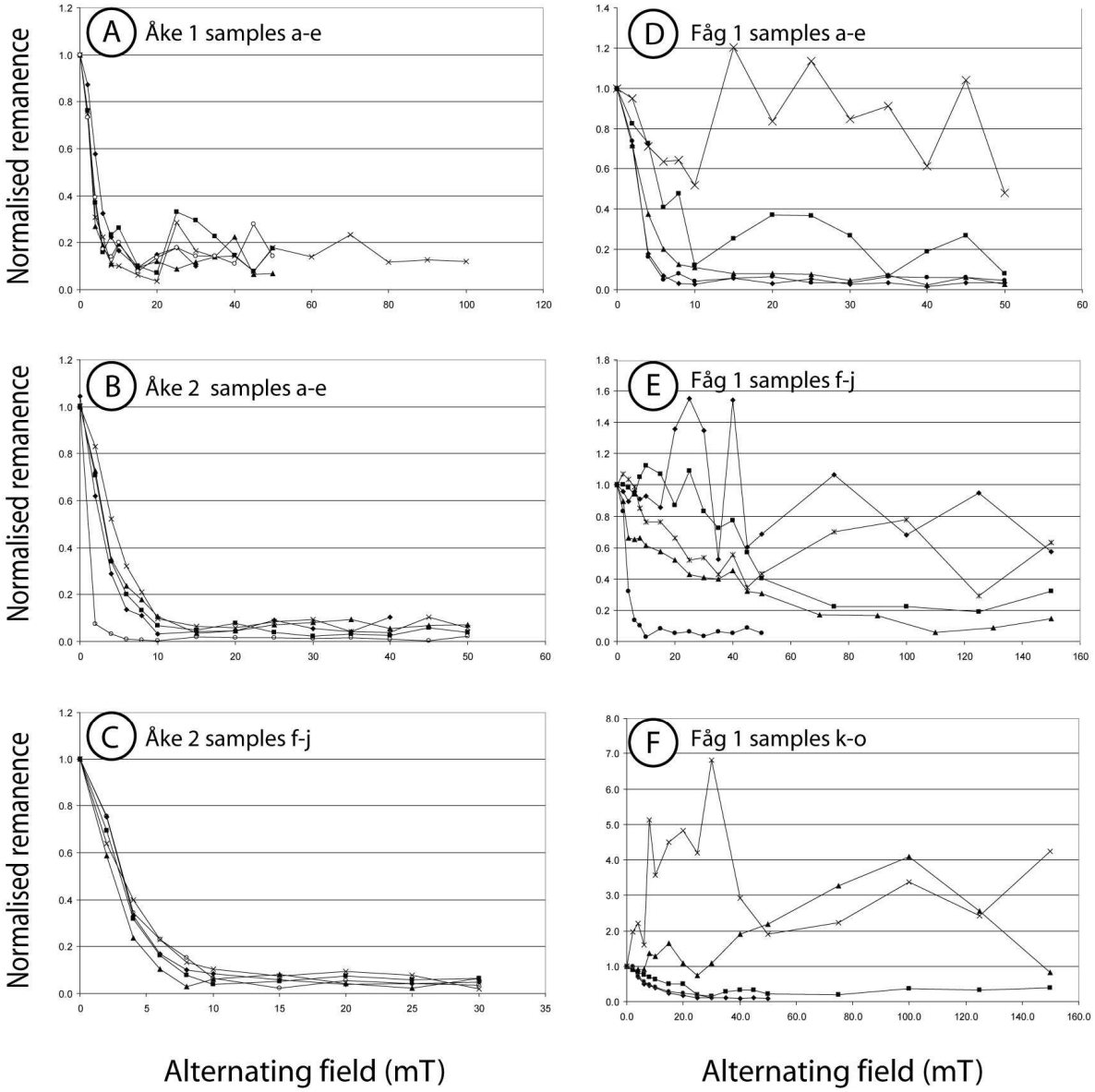

Figure 9. Alternating Field demagnetization curves for the investigated outcrops. T=Tesla. The curves have been normalized with their initial intensities (J_s/J_0). **NOTE DIFFERENT SCALE ON Y- and X- AXES.**

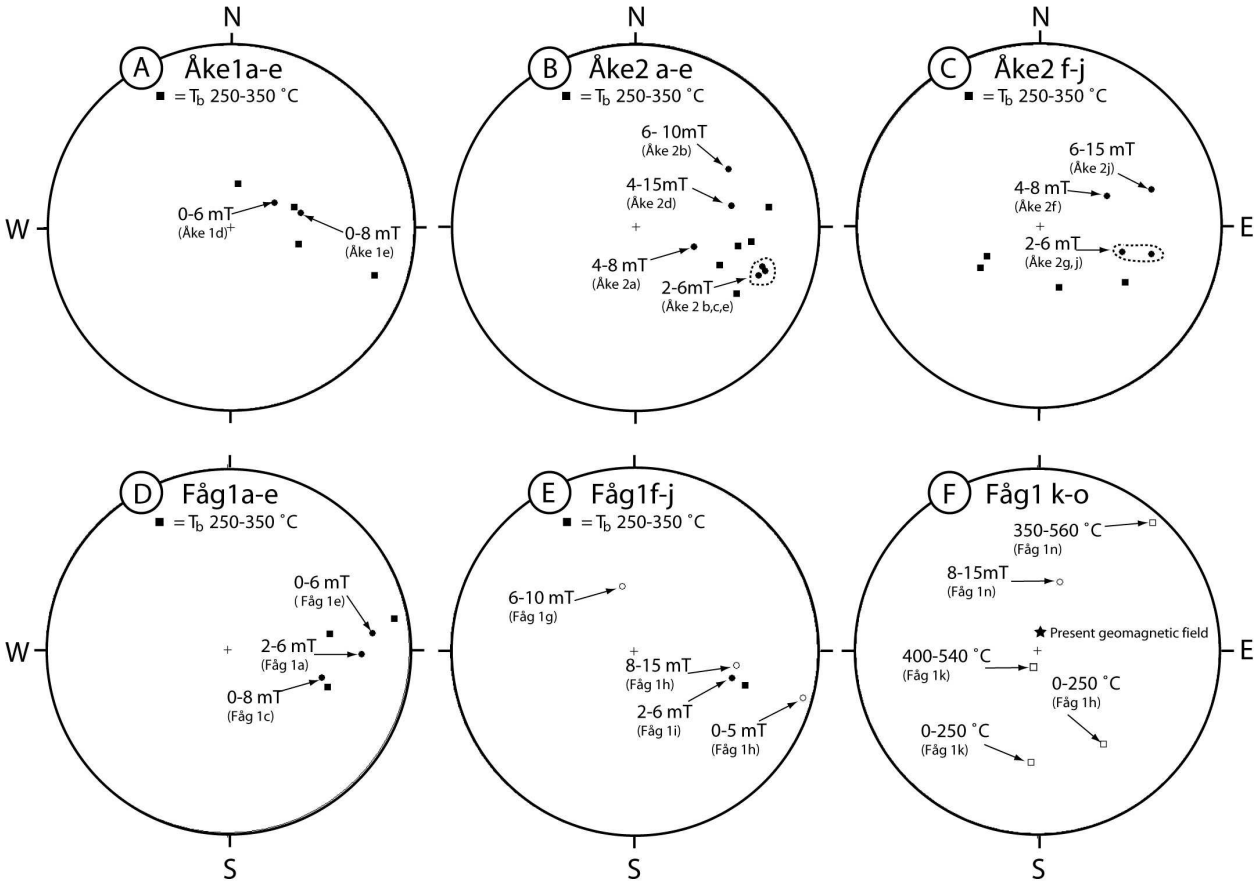

Figure 10. ChRM-directions plotted in stereograms (Wulf-projection). Boxes indicate thermal demagnetization. Circles indicate AF-demagnetization. Open boxes or circles indicate negative inclination, solid boxes or circles indicate positive inclination. The star shows the direction of the present geomagnetic field. T_b is blocking temperature.

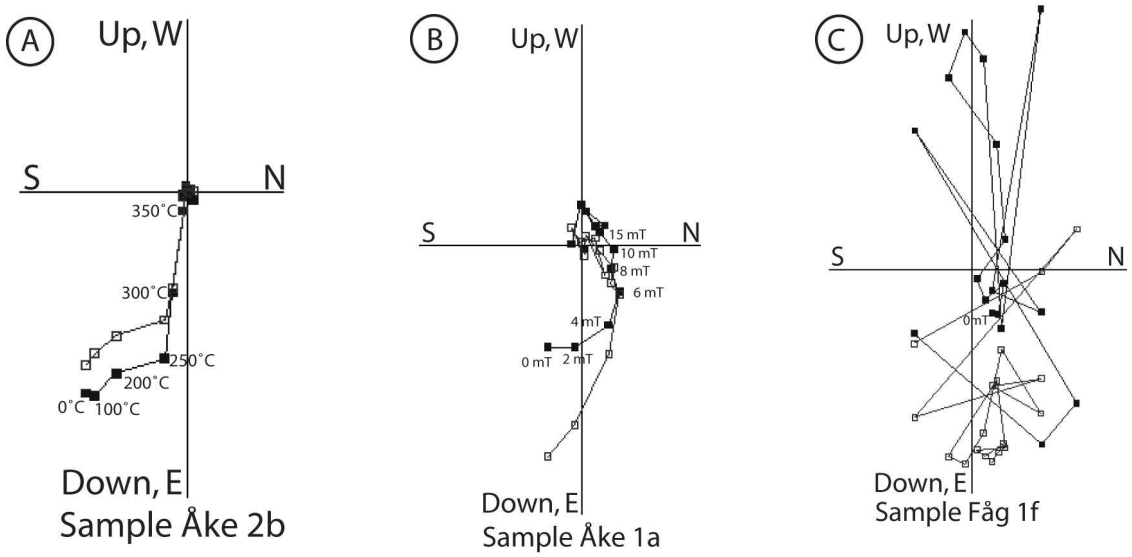

Figure 11. Examples of Zijderveld projections discussed in the text. A) is an example of two directions. The low T (0-250 ºC) direction is likely secondary NRM. The high T (250-350) ºC is primary NRM. B) is likely an example of over- lapping coercivity spec-tras. C) is an example of chaotic behavior. T=Tesla.

7.1.3 Correlation of VGP with Paleomagnetic Poles

From the ChRM-directions in Figure 10, one group was identified with Fisher statistics. This group was named Group 1 and is shown in Figure 12. The directional data for this group has been summarized in Table 2. As Table 2 shows, most directions were obtained from the outcrop Åke 2, but some directions in the identified group were also obtained from outcrops Åke 1 and Fåg 1.

From this group of ChRM-directions one VGP was calculated, which can be seen in Table 3. The VGP had a paleolatitude /paleolongitude (Plat/Plong) of 20.1°/92.7°. This VGP does not correlate to any of the reported paleomagnetic poles in Table 4. If polar reversal is considered, the calculated VGP have the following Plat/Plong: -20.1/272.7. This location is similar to poles with an age of ~950 Ma in Table 4.

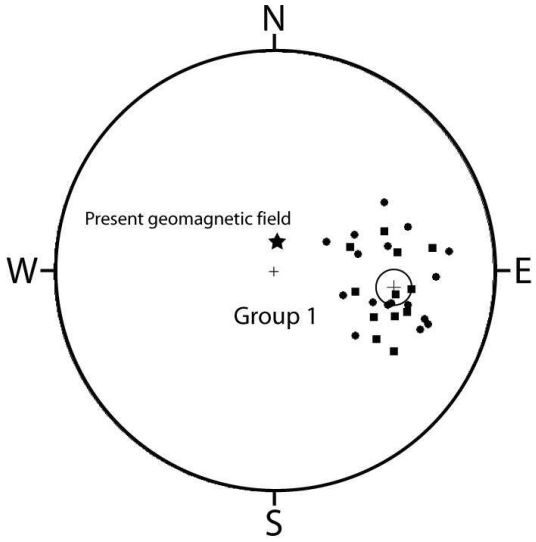

Figure 12. Group 1s ChRM-directions projected in a sterogram (Wulf-projection). Solid circles=AF-demagnetization. Solid boxes=Thermal demagnetization. The circle and cross indicates α 95, which is the 95% cone of confidence.

Table 2.

Site (sample)	Number of drill cores/ number of samples	Number of demagnetizations directions	Decl.	Incl.	α 95, *95% cone of confidence*	K, *Fischer precision parameter*
Åke 1 (a-e)	5 / 10	4	80.2	61.9	11.1	70.04
Åke 2 (a-e)	5 / 10	11	99.3	39.9	10.6	19.37
Åke 2 (f-j)	5 / 10	6	100.3	48.2	16.4	17.74
Fåg 1 (a-e)	5 / 10	5	94.0	35.6	14.4	29.35
Fåg 1 (f-j)	5 / 10	2	105.9	40.2	16.3	22.9
Fåg 1 (k-o)	5 / 10	-	-	-	-	-
Sum(Mean)	30 / 60	28	(97.1)	(44.3)	(6.3)	(19.93)

Table 2. Table of the demagnetization directions obtained from the samples. Decl = Declination. Incl = Inclination. α 95 = 95% cone of confidence. K = Fischer precision parameter.

Table 3.

Component	**Decl**	**Incl**	**N**	**R**	**K**	**α95**	**VGP-lat**	**VGP-long**	**D_p/D_m**
Group 1	97.1	44.3	28	26.65	19.93	6.3	20.1	92.7	5/7.9

Table 3. The table show the directions of the calculated VGP (Virtual magnetic Pole). Decl=Declination. Incl= inclination. N, R, K are Fisher precision parameters. α 95 is the 95% cone of confidence. D_p/D_m are the values of the ovals of 95% confidence.

Table 4.

Rock formation	Age (Ma)	Plat	Plog	D_p	D_m	Reference
Akujarvi quartz-diorite	~1925	41.3	245.5	4.0	7.0	Pesonen et al., 1991
Menesjarvi granulite	~1925	33.8	232.2	4.7	8.6	Pesonen et al., 1991
Bo diorites	1740-1880	59.0	188.0	6.0	10.0	Pesonen et al., 1991
Keuruu dykes	~1880	45.4	218.4	4.0	7.0	Pesonen et al., 1991
Nordingrå Örnsköldsvik dykes	1850±130	66.2	223.3	21.6	27.3	Pesonen et al., 1991
Tärendö gabbro 2	1757±43	44.9	229.6	3.3	5.4	Pesonen et al., 1991
Notträsk gabbro	1840±390	42.6	219.7	2.4	4.1	Pesonen et al., 1991
Sangis gabbro	1840±390	46.5	205.4	2.0	3.4	Pesonen et al., 1991
Store Lulevattnet gabbro	1530-1770	40.0	222.1	11.0	19.0	Pesonen et al., 1991
Vaasa Dolerite Dykes	1268	7	164	3.2	5.5	Neuvonen, 1966
Laanila-Ristijärvi Dykes	1042	-2	212	12	21	Mertanen et al., 1996
Båtsfjord dykes	650	40.6	108.2	5.1	6.7	Kjöde, 1980
Lösen Fäjö	946	-23	249	2.7	5.4	Pachett & Bylund, 1977
Bräkne Hoby	949	-22	252	3.1	6.1	Pachett & Bylund, 1977
Fen Complex	583	55	155	8	13	Meert et al., 1998
Alnö Complex A (R)	545-589	12.9	269.3	7.7	15.3	Piper, 1981
Sredniy Dykes	525-580	72.9	94.7	4.2	4.4	Torsvik et al., 1995
Torneträsk Formation	535	56	116	12	15	Torsvik & Rehnström, 2001
Andrarum Limestone	500	52	111	7	10	Torsvik & Rehnström, 2001

Table 4. Selected paleopoles from the Baltic shield during the time interval 1925-500 Ma. Plat = paleolatitude, Plong = paleolongitud. D_p and D_m are the values of the ovals of 95% confidence.

7.2 Köningsberger Ratios, NRM-intensities and Susceptibility

The measured and calculated rock magnetic properties, Köningsberger ratios (Q), NRM-intensities and susceptibility have been compiled in Figure 13 and Table 5.

The mean site susceptibility values seen in Table 5 are highest in outcrop Åke 2. The Fåg 1 outcrop has lowest susceptibilities compared to Åke 1 and Åke 2. In Fåg 1 a-e an exceptionally high susceptibility was recorded. However, the NRM-intensity and Q-value were not exceptionally large and the high susceptibility can be ascribed a higher concentration of pyrrhotite.

In all sampled outcrops, there is a strong correlation between NRM-intensities and Q-values. In samples with low Q-values and NRM-intensities, such as samples from outcrop Fåg 1, gave little or no paleomagnetic data, whereas outcrops with high Q-values and NRM-intensities, such as Åke 2 gave stable directions.

7.3 Thermomagnetic curves

The results from the thermomagnetic measurements are shown in Figure 14.

Sample Åke 1c (Figure 14a) showed reversible curves during heating and cooling, which made it possible to determine the Curie temperature (T_C) from the sample. The T_C was determined to 325 °C. This T_C corresponds very well to monoclinic pyrrhotite, which has a T_C of 310-325 °C (Dekkers, 1989). Another indication that sample Åke 1c carried monoclinic pyrrhotite was the absence of the so-called λ-transition. The λ-transition is typical for hexagonal pyrrhotite (antiferrimagnetic) and it represents a transition between hexagonal and monoclinic pyrrhotite. In thermomagnetic curves, the λ-transition is seen as an increase in susceptibility at 200-210 °C (depending on the composition of the pyrrhotite).

Sample Åke 2b (Figure 14b) was very similar to the curve of sample Åke 1c (described above). When cooling started at 410 °C (the blue curve) it showed higher susceptibilities compared to the heating phase.

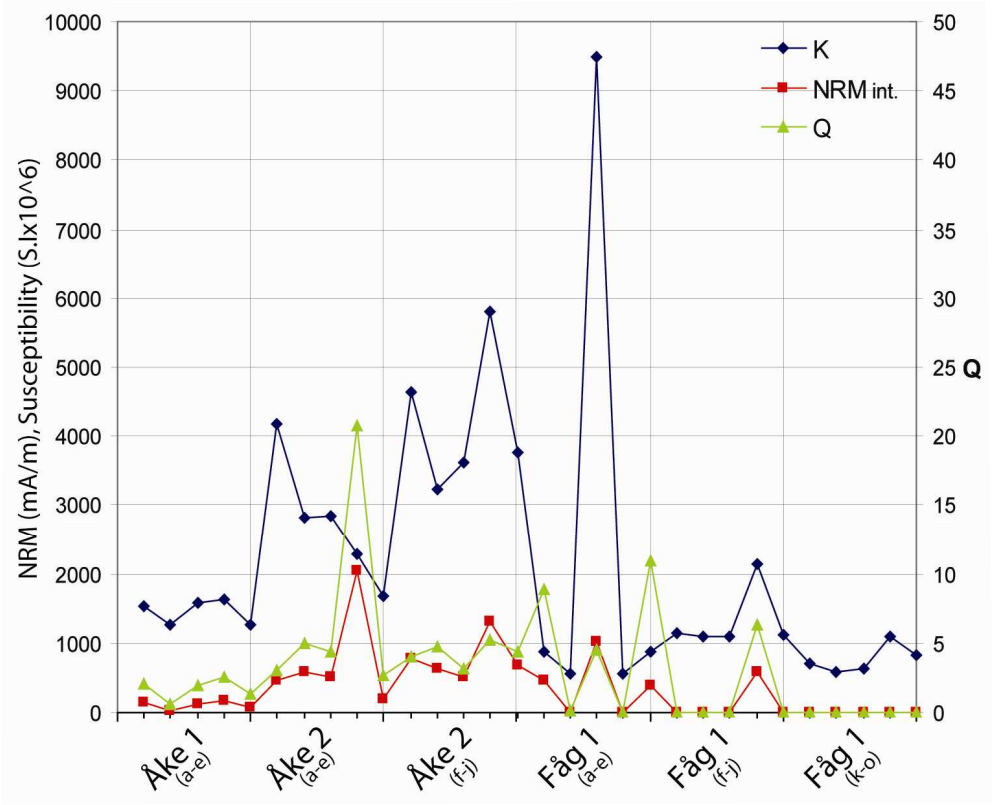

Figure 13. The diagram shows susceptibility (K), NRM-intensities (NRM-int) and Köningsberger ratios (Q). All samples are represented in the diagram. Samples with low NRM-int. and Q values gave less stable paleomagnetic data. Please note that Q-values (green line) are plotted on a secondary Y-axis.

Table 5

Site (sample)	**Intensity,** *mean value and (range) (mA/m)*	**Q,** *mean value and (range)*	**Susceptibility** *(SI*10^{-3}),* *Mean value and (range)*
Åke 1 (a-e)	110 (170-31)	1.70 (2.58-0.60)	1.44 (1.62-1.26)
Åke 2 (a-e)	760 (2000-200)	7.18 (20.77-2.68)	2.76 (4.18 -1.67)
Åke 2 (f-j)	780 (1300-500)	4.30 (5.24-3.14)	4.21 (5.18 -3.24)
Fåg 1 (a-e)	370 (1000-0.27)	4.85 (10.87-0.011)	2.46 (9.48 -0.55)
Fåg 1 (f-j)	120 (600-0.27)	1.28 (6.36-0.005)	1.32 (2.14 -1.09)
Fåg 1 (k-o)	0.54 (1.2-0.07)	0.02 (0.03-002)	0.77 (1.10 -0.59)

Table 5. Magnetic data from all sampling localities. Q=Köningsberger ratio, formula Q=(NMR)/χH. Where χ=susceptibility and H the geomagnetic field. H= 41.701A/m (National Geophysical Data Centre, 2006).

The cooling curve indicates that a mineralogical reaction has occurred in the sample. The most likely reaction to have occurred is oxidation of pyrrhotite to magnetite. Because of this reaction, the curve is not fully reversible.

In sample Fåg 1c (Figure 14c) the susceptibility of the sample increases during heating (red curve) at temperatures 280-310 °C and then it rapidly decreases to reach a minimum at ~320 °C. The heating curve reaches a new minima at ~580 °C. During cooling, the curve shows irreversible behavior. The irreversible behavior is seen in the temperature interval ~310-520 °C and ~50-300°C for the cooling curve. This behavior can be explained by the presence of monoclinic pyrrhotite. The first susceptibility minimum indicates monoclinic pyrrhotite. At increased temperature, pyrrhotite oxidizes to magnetite, which has a T_C of ~580 °C. This oxidation explains the second susceptibility minima and the irreversible behavior of the curve.

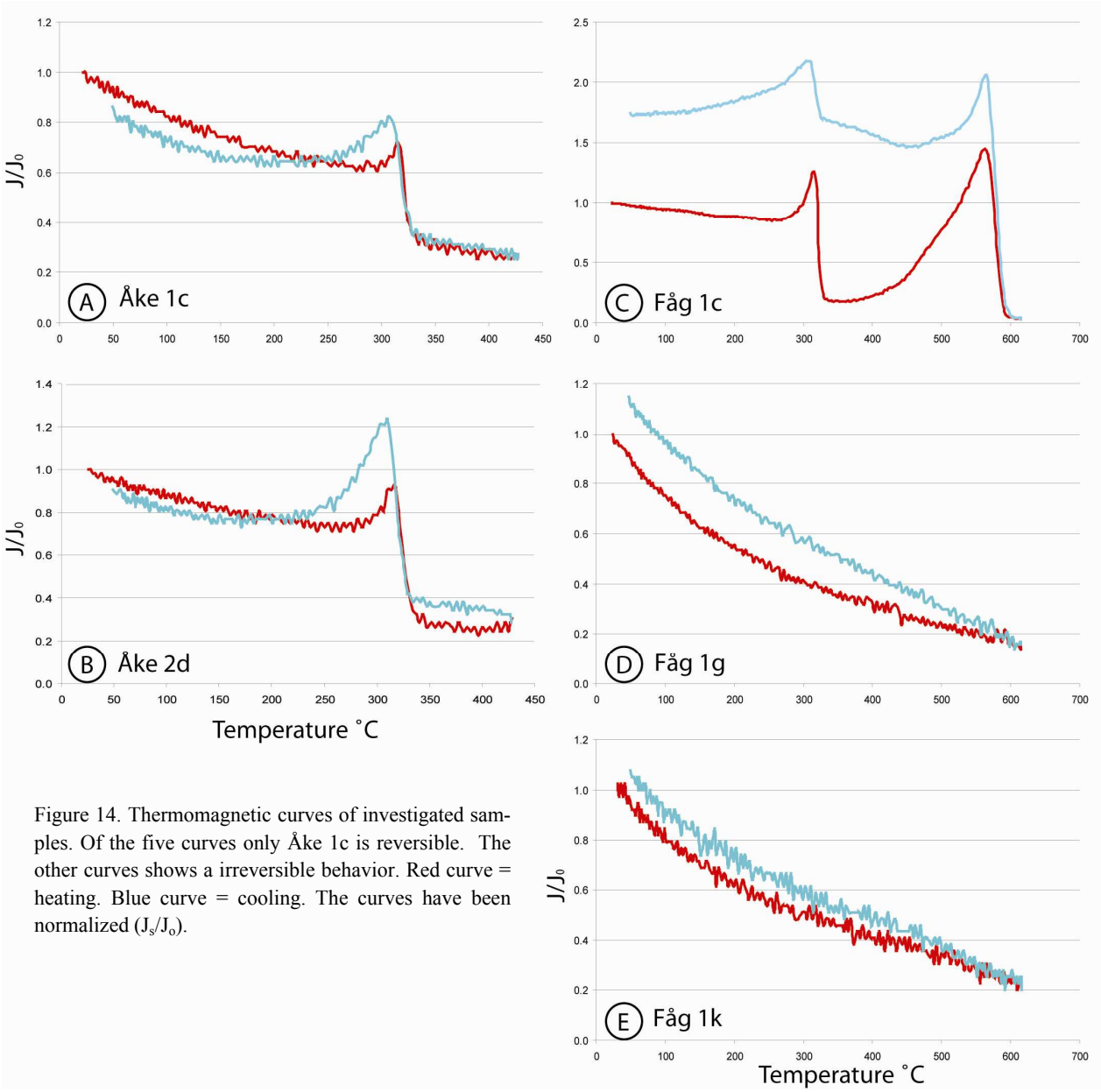

Figure 14. Thermomagnetic curves of investigated samples. Of the five curves only Åke 1c is reversible. The other curves shows a irreversible behavior. Red curve = heating. Blue curve = cooling. The curves have been normalized (J_s/J_o).

The thermomagnetic curves of sample Fåg 1g and 1k are irreversible which indicates that a mineralogical reaction has occurred (Figure 14d-e). From the curves, it is not possible to determine what kind of mineral(s) that is present in the samples. The samples will be discussed further in chapter 8.

7.4 Optical and SEM-results

Optical and SEM-results have been summarized in Table 6, the table also shows which samples that where optically and (or) SEM-investigated. In the sections below the major phases will be described in order of abundance.

7.4.1 Silicate Phase

The dominating rock forming mineral in all investigated samples was amphibole. The amphibole was generally fine to medium grained. The fine grain sizes dominated in samples from Åke 1 and Åke 2 and the medium grain sizes in samples Fåg 1f-j. In Fåg 1a-e and Fåg 1k-o the grain size was more intermediate (fine to medium grained).

In samples from Åke 1 and Åke 2, the amphibole had a green color, whereas in samples from Fågelberget the color varied between green and blue-green. A common texture found in the amphibole was crystallographically orientated inclusions of ilmenite (Figure 15a). This texture was different between samples from Fåg 1 and Åke 1 and 2, which can be seen in Figure 15a and 15b respectively. In samples from Fåg 1a-e the amphibole and occasionally the biotite contained halos, which indicated radiogenic decay of possibly xenotime, zircon or monazite (see Table 6).

Plagioclase was abundant in samples from Åkerberg and in some samples microcline was also pre-

Table 6.

	Out-crop	Sample	Optical	SEM	Silicate phases	Opaque phases	% Opaque	Comment
Åkerberg	Åke 1	Åke1a	-	-	-	-	-	Ore zone
		Åke1b	-	-	-	-	-	
		Åke1c	X	X	Am, Plg, Ap, (Bi, Qz,, Px, Zr)	Il, Ph, (Cp, Arp, Se, Sph, G)	10-15	
		Åke1d	X	-	Am, Plg, Qz, Ap, (Bi, Chl, Px)	Il, Ph, (Cp, Arp)	<10	
		Åke1e	-	-	-	-	-	
	Åke 2	Åke2a	-	-	-	-	-	Middle part of outcrop
		Åke2b	X	-	Am, Plg, Ap, (Bi)	Il, Ph, (Arp, Cp)	10-15	
		Åke2c	-	-	-	-	-	
		Åke2d	-	-	-	-	-	
		Åke2e	X	X	Am, Plg, Mc, Ap, (Bi)	Il, Arp, Ph, (Cp)	10-15	
		Åke3a	X	-	Am, Plg, Ap, (Bi)	Il, Ph, (Cp)	<10	Lower part of outcrop
		Åke3b	-	-	-	-	-	
		Åke3c	X	-	Am, Plg, Mc, Ap, Bi	Il, Ph, (Arp, Cp)	10-15	
		Åke3d	X	X	Am, Plg, Bi, Ap	Il, Ph, (Cp)	10-15	
		Åke3e	-	-	-	-	-	
Fågelberget	Fåg 1	Fåg 1a	X	-	Am, Bi, Plg, (Px)	(Ph, Cp)	<1	Bottom layer
		Fåg 1b	-	-	-	-	-	
		Fåg 1c	-	-	-	-	-	
		Fåg 1d	X	X	Am, Plg,	(Ph, Cp)	<<1	
		Fåg 1e	-	-	-	-	-	
		Fåg 1f	-	-	-	-	-	Middle layer
		Fåg 1g	-	-	-	-	-	
		Fåg 1h	X	X	Am, Qz, Px (Chl, Zr)	Il , Ru,	10-15	
		Fåg 1i	X	X	Am, Qz, Px (Chl)	Il, Ph,	10-15	
		Fåg 1j	X	X	Am, Px (Chl)	Il	~5	
		Fåg 1k	X	X	Am, Plg, Ep/Cz	Il, (Ph)	<2	Contact (of bottom and middle layer)
		Fåg 1l	-	-	-	-	-	
		Fåg 1m	-	-	-	-	-	
		Fåg 1n	X	X	Am, Plg, Px (Chl, Ep/Cz)	Il, (Ph)	<8	
		Fåg 1o	-	-	-	-	-	

Table 6. Summary of optical and SEM investigations. ( ) = Minor phase, X = investigated, - = not investigated

Silicate phases: Am= Amphibole / Ap= Apatite / Bi= Biotite / Chl= Chlorite / Ep-Cz= Epidote and (or) Clinozoisite / Mc= Microcline / Plg= Plagioclase / Px= Pyroxene / Qz= Quartz / Zr=Zircon

Opaque phases: Arp= Arsenopyrit / Ba= Barite / Cp= Chalcopyrite / G= Gold / Il= Ilmenit, / Ph= Pyrrhotite /Ru= Rutile / Se= Scheelite / Sph= Sphalerite

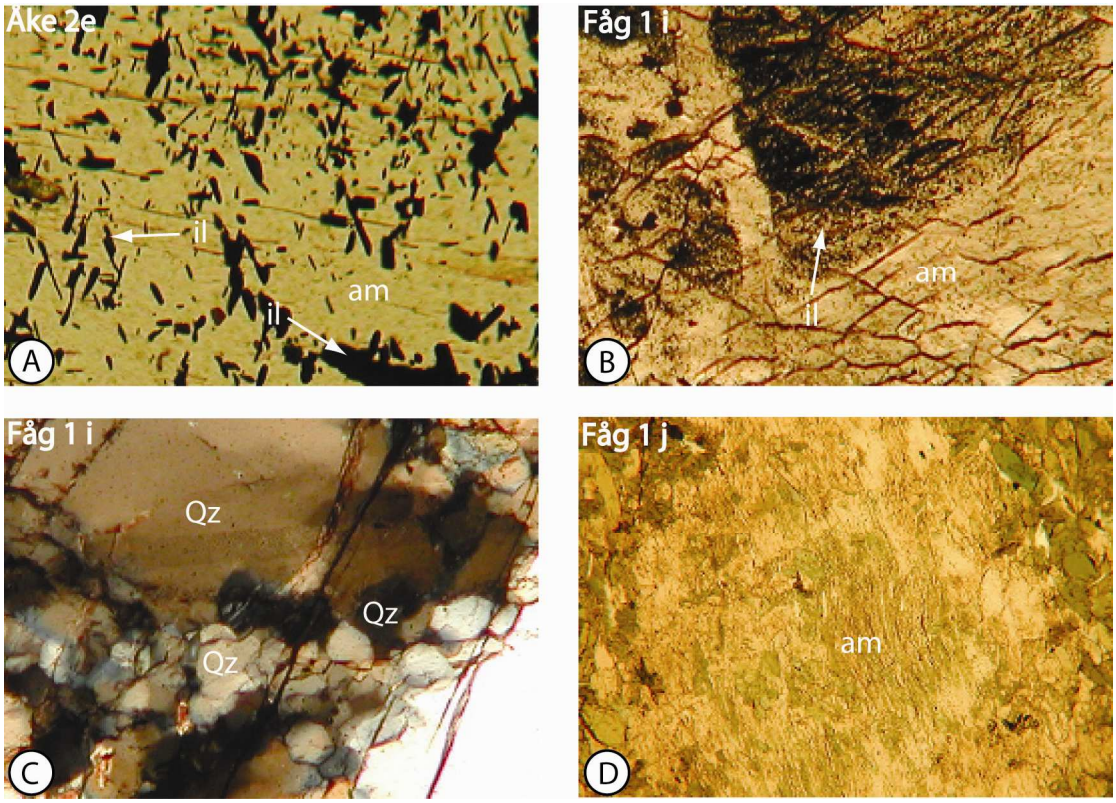

Figure 15. All photos are taken in plane polarized light except C) which was taken in cross polarized light. A) shows crystallographically orientated ilmenite grains in an amphibole grain, the texture is typical for samples from Åkerberg. B) shows dirty replacement or exsolution of ilmenite in an amphibole grain, the texture is typical for samples for samples from Fågelberget. C) Recrystallized quartz grains. D) Uralite.

sent. In most cases, both plagioclase and microcline were strongly sericitized. In samples from Fåg 1a-e and k-o the plagioclase and amphibole occurred in rather similar amounts, but the plagioclase showed only minor sericitization. A different plagioclase alteration was observed in one sample from site Fåg 1. This alteration was interpreted as a replacement of plagioclase by epidote and (or) clinozoistite.

Pyroxene, which is expected to constitute a major phase in an unaltered gabbro, was scarce or absent in samples from Åkerberg. Replacement of pyroxene by amphibole (in a replacement texture called uralitization) was also scarce, and it was only observed in samples from Åke 1. In samples from Fåg 1, pyroxene was more common. The pyroxene occurred as small grains dispersed in thin sections. In some samples from Åke 1, Åke 2 and Fåg 1 the amphibole occurred as fine grained fibrous aggregates (generally called uralite) (Figure 15d), which can be associated with the replacement of pyroxene by amphibole (Deer et al., 1992).

In thin sections from Åke 1 and Fåg 1f-j, quartz was abundant. Quartz occurred as larger grain aggregates that were partly recrystallized (Figure 15c).

Apatite was most abundant in Åke 1 and Åke 2 where it occurred as sub- to euhedral grains dispersed in the thin sections. In samples from Fåg 1, apatite was scarce.

7.4.2 Opaque Phases

In the Chapter 4, it was mentioned that ferrimagnetic minerals such as pyrrhotite and magnetite, carried the NRM of a rock. A major goal during the optical and SEM-investigations was therefore to identify the opaque phases in thin sections to see if they consisted of ferrimagnetic minerals. Figure 16a-e shows SEM-images taken during the investigations. In the text below, these figures are referred together with Appendix 1. In Appendix 1, the spectrum of the analyzed grains can be seen.

For each investigated sample, the amounts of opaque phases were estimated. The numbers given here, and in Table 2 are therefore not absolute, but they serve as an indication of the relationship between the sites.

The amount of opaque phases was considerably higher in samples from Åke 1 and Åke 2 compared to Fåg 1. In all samples except samples from Fåg 1a-e ilmenite dominated among the opaque minerals. Ilmenite occurred as larger anhedral grains ranging in size between 0.2-1 mm (Figure 16a and Appendix 1). It was common that larger ilmenite grains had inclusions of small (<0.02 mm) pyrrhotite grains. In site Fåg 1f-j the ilmenite was altered to rutile (Table 2). Rutile also appeared as smaller grains along ilmenite grain boundaries (Figure 16b and Appendix 1).

In Åke 1 and Åke 2, ilmenite also appeared as

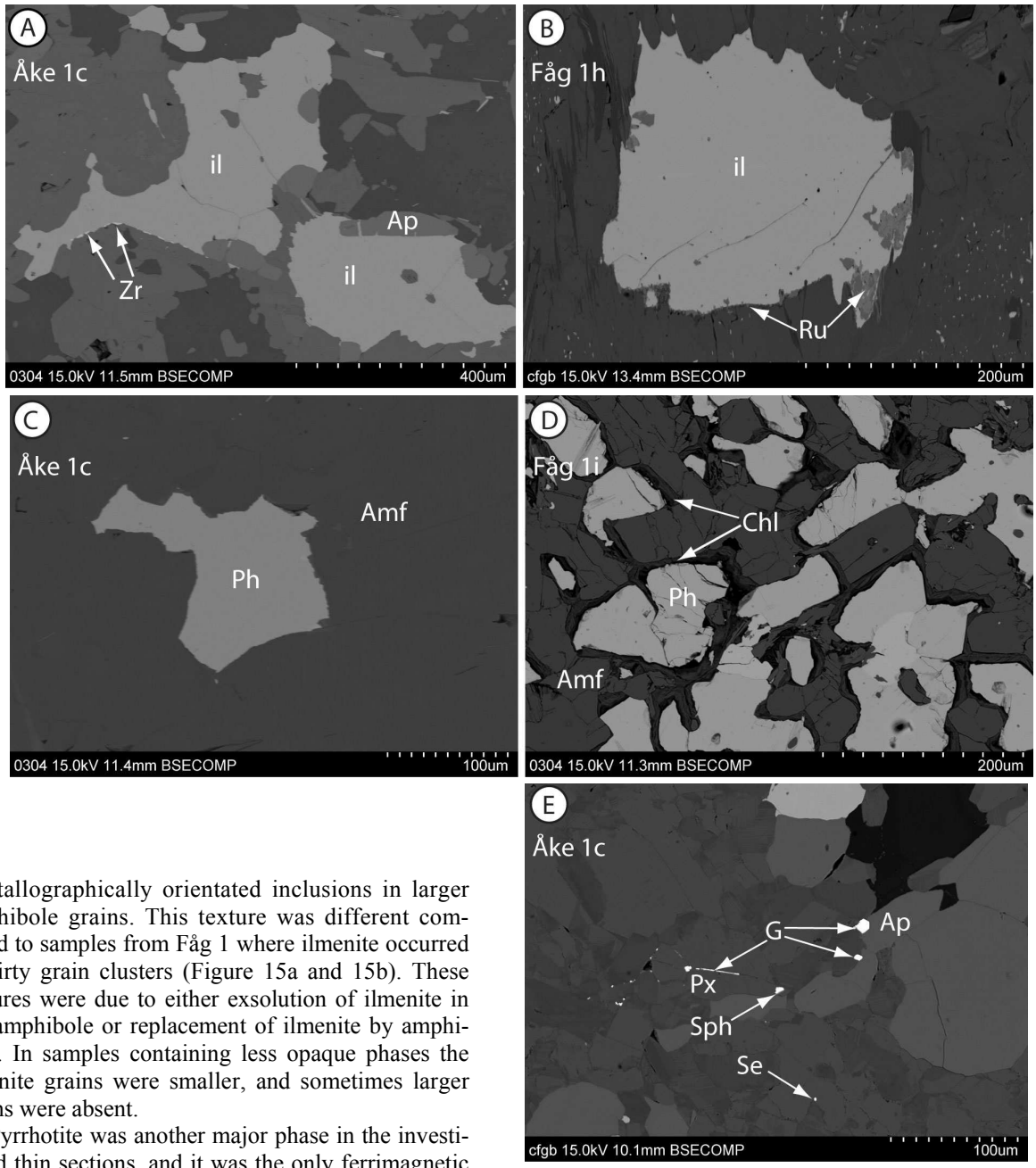

Figure 16. SEM-photos of selected opaque minerals. A. Ilmenite grain occurring together with apatite. Note the small grains of zircons. B. Ilmenite grain with inclusions of rutile and small rutile grains at ilmenite grain boundaries. C. Pyrrhotite grain in an amphibole matrix. D. Cluster of pyrrhotite grains in amphibole matrix. Note the chlorite coronas. E. Gold and gold associated minerals such as sphalerite and scheelite. The gold occurs in a small fracture of a pyroxene grain and together with an apatite grain. For SEM-analysis spectra see Appendix 1.

crystallographically orientated inclusions in larger amphibole grains. This texture was different compared to samples from Fåg 1 where ilmenite occurred as dirty grain clusters (Figure 15a and 15b). These textures were due to either exsolution of ilmenite in the amphibole or replacement of ilmenite by amphibole. In samples containing less opaque phases the ilmenite grains were smaller, and sometimes larger grains were absent.

Pyrrhotite was another major phase in the investigated thin sections, and it was the only ferrimagnetic mineral observed during optical and SEM-investigations (Figure 16c and Appendix 1). The amount of pyrrhotite was considerably higher in Åke 1 and Åke 2 compared to samples from Fågelberget.

Pyrrhotite occurred as inclusions in larger ilmenite grains, but it was more commonly dispersed in other minerals. The grain sizes of pyrrhotite varied between <0.2mm and 0.2-1 mm. The smaller grain sizes (<0.2 mm) were more common. Additional phases occurring together with pyrrhotite were chalcopyrite and arsenopyrite, but arsenopyrite also occurred independently.

In samples from Åke 1 and Åke 2, pyrrhotite showed no signs of alteration or reaction with the silicates. In Fåg 1f-j however, a cluster of pyrrhotite grains showed a corona texture which consisted of chlorite (Figure 16d, and Appendix 1).

Additional opaque phases found during optical and SEM investigations were gold and gold-associated minerals such as scheelite ($CaWO_4$) and sphalerite (Figure 16e and Appendix 1). These minerals were observed in Åke 1. In site Fåg 1 f-j barite ($BaSO_4$) was found.

8 Discussion

8.1 The Carriers of NRM in the Outcrops

Three outcrops were sampled, Åke 1, Åke 2 and Fåg 1. These outcrops were sampled as they represented different parts of the investigated meta-gabbro. The outcrops were also suitable for the aims of this paper, which were to quantify the magnetic properties of the ore zone in the Åkerberg gold deposit and to investigate a possible block movement indicated in the southern part of the open pit. In order to proceed with these investigations, the carriers of NRM in the outcrops first have to be quantified.

When comparing the (AF- and Thermal) demagnetization results, thermomagnetic measurements, rock magnetic data such as Q-values, NRM-intensities and susceptibility presented in Chapter 7, it becomes apparent that the different outcrops share some magnetic properties, but that there are also important differences between them.

Looking at different demagnetization trends may help explaining these similarities and differences. Three different thermal demagnetization trends have been exemplified in Figure 17. Together with other measurements, such as thermomagnetic curves and optical and SEM-investigations, it is possible to determine the carriers of NRM in the samples from these trends. It is important to mention that these trends were also observed from the AF-demagnetization results.

Thermal and AF-demagnetization of the outcrops Åke 1 and Åke 2 show similar demagnetization trends. In Figure 17, Trend 1 describes their thermal demagnetization behavior. During demagnetization, the curves decreased in susceptibility between 200-350 ºC and during AF-demagnetization the curves decreased between 0-10 mT. Thermomagnetic measurements of one sample from Åke 1 and one sample from Åke 2 showed that the carrier of NRM was monoclinic pyrrhotite (Figure 14a-b). The thermal demagnetization curves indicate that the majority of the pyrrhotite grains are larger than 5 µm, as grain sizes smaller than this would shift the demagnetization curve to the right. In other words, a smaller grain size (<5 µm) would result in a less convex demagnetization curve with an intensity decrease that ended at lower demagnetization temperatures (Dekkers, 1989). This interpretation is consistent with optical and SEM-results where pyrrhotite was observed as an abundant opaque phase.

Trend 1 is also observed in samples from Fåg 1. The samples that showed this trend had a strong intensity decrease between 200-350 °C (Thermal demagnetization) or between 0-10 mT (AF-demagnetization) (Figure 8d-e and Figure 9d-e respectively).

Thermomagnetic measurement of site Fåg 1 showed that monoclinic pyrrhotite was the ferrimagnetic phase (Figure 14c). This interpretation is consistent with the T_N of pyrrhotite, which is 310-325 °C (Dekkers, 1989). Abundant pyrrhotite was also found during optical and SEM-investigations (Table 2, sample Fåg 1i). It is therefore most likely that monoclinic pyrrhotite is a carrier of NRM in Fåg 1.

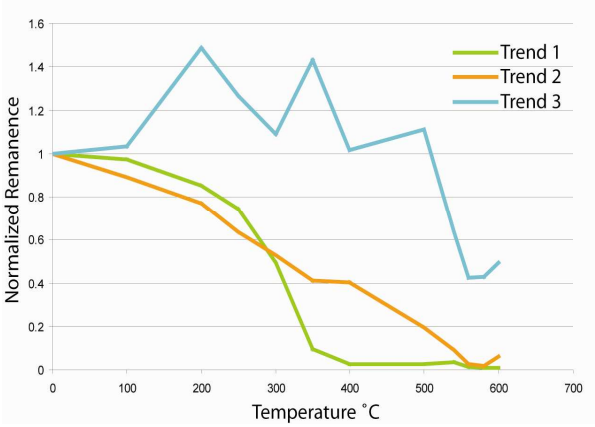

Figure 17. The figure shows three different demagnetization trends observed during thermal demagnetization.

Demagnetization Trend 2 in Figure 17 was observed in some samples from outcrop Fåg 1. In Figure 8f (samples Fåg 1f-j), this trend was characterized by a continued intensity decrease during demagnetization up to temperatures of 540-580 °C or alternating fields of 30-40 mT. In Figure 8e (samples Fåg 1k-o) this trend was not as clearly indicated during thermal demagnetization, but during AF-demagnetization the trend was clearer (Figure 9e). To assess what mineral is responsible for the behavior, a brief review of the ChRM-directions obtained from these samples is useful. ChRM-directions from these samples were stable in an interval of higher coercivities or blocking temperatures, generally in alternating fields between 8-15 mT or temperatures of 350-560 °C.

During optical and SEM-investigations minor or no pyrrhotite was observed in samples that gave stable ChRM-directions in these intervals, nor is the T_N (310-325 °C) of pyrrhotite high enough to explain the high T_b of these samples. The ferrimagnetic phase is more likely magnetite, which has a T_C of 580 ºC (Dunlop & Özdemir, 2001). The magnetite T_C is consistent with the observed low intensities in site Fåg 1 (Figure 8f) at demagnetization temperatures of 580 °C.

The amount of magnetite is interpreted as low, since these samples showed low susceptibility-values during measurements (using Peters & Dekkers, 2003, conclusion that susceptibility can be used to assess ferrimagnetic grain concentrations). For example, the mean susceptibility of Fåg 1f-j and Fåg 1k-o was 1.32 and 0.77, respectively (Table 5). These values can be compared to the mean values of Åke 1 and Åke 2a-e and f-j, which were 1.44, 2.76, and 4.30 respectively (Table 5).

The low susceptibilities also explain the paramagnetic behavior of samples that contained magnetite during thermomagnetic measurements (Figure 14d-e). Because of the low magnetite concentration, it is likely that the paramagnetic minerals obscure the behaviour of magnetite in the samples. This low susceptibility also explains why no magnetite was observed during optical and SEM investigations.

From Trend 2 it cannot, however, be excluded that pyrrhotite contributes to some of the NRM. This conclusion can be made from the curves behavior between 0-325 ºC.

The third demagnetization trend in Figure 17 was observed in outcrop Fåg 1. The trend can be described as irregular or chaotic. Samples in Fåg 1 that showed this behavior all had low susceptibilities and NRM-intensities, which can be seen in Figure 13. Trend 3 thus indicates a paramagnetic behavior.

To summarize the results, in the outcrops Åke 1 and Åke 2 monoclinic pyrrhotite is the carrier of NRM. Monoclinic pyrrhotite was also the carrier of NRM in some samples from Fåg 1, but this outcrop also showed evidence of magnetite.

8.2 Implications of the ChRM-directions

The ChRM-directions obtained from the principal component analysis have been excluded from the discussion so far. This data, however, reveals important differences between the ChRM-directions obtained from samples that carried monoclinic pyrrhotite and ChRM-directions obtained from samples that carried magnetite. Pyrrhotite yielded ChRM-directions with positive inclination. Magnetite yielded ChRM-direction with negative inclination. To explain the different ChRM-directions, the intrinsic properties of pyrrhotite and magnetite must be assessed and placed in their geological context.

The investigated meta-gabbro has been exposed to metamorphic conditions of lower amphibolite facies (Lundström & Antal, 2000). Dunlop & Özdemir (2001) reports that metamorphism of higher greenschist to lower amphibolite facies leads to thermal overprinting of ferrimagnetic minerals. During thermal overprinting minerals are heated and at temperatures greater than the Tb of the mineral the NRM disappears. During cooling, the minerals acquire a new NRM when Temperature reaches below the Tb of the mineral. In fact, the thermal overprinting is similar to how thermal demagnetization works. There is however, one important difference. In natural conditions, the Tb is considerably lower for magnetite and pyrrhotite compared to laboratory experiments, since the Tb is time dependent. The natural Tb can be as much as 200 ºC below the laboratory Tb (Dunlop & Özdemir, 2001).

In the investigated meta-gabbro, pyrrhotite and magnetite are the carries of NRM. These minerals have a T_N = 310-325 ºC and T_C = 580 ºC respectively. If this data is put into the metamorphic conditions of the Åkerberg area, it becomes clear that the primary NRM of pyrrhotite cannot survive the metamorphic conditions reported from the area.

As shown in Figure 10 samples that contained pyrrhotite in Fåg 1 yielded similar directions as samples from Åke 1 and Åke 2, which all contained abundant pyrrhotite. This similarity means that Fåg 1, Åke 1 and Åke 2 could have acquired their ChRM-directions at the same event.

In chapter, 7.1.3 the VGP was determined from these directions. The calculated VGP did not correlate to any of the reported paleopoles. But considering polar reversal, the calculated pole showed correspondence to paleopoles with an age of ~950 Ma. The calculated VGP can, however, not be considered a paleopole for statistical reasons. Any attempt to correlate it with reported paleopoles should therefore be done with caution.

The ChRM-directions from the magnetite component are seen as open circles and boxes in Figure 10. These directions are too scattered and too few have high Tb or coercivity for VGPs to be calculated. It is therefore impossible to determine if the magnetite grains carry primary NRM or NRM acquired subsequent to rock formation. It is, however, very likely that the ChRM-directions obtained from magnetite are older compared to the ChRM-directions obtained from pyrrhotite containing samples. This conclusion can be made because the higher T_b of magnetite indicates that this mineral is more resistant to overprinting. This relationship also implies that the NRM carried by magnetite in the meta-gabbro is most likely older compared to the NRM carried by pyrrhotite.

8.3 Investigation of Block Movement

One of the objectives with this thesis was to investigate possible block movement in the shear zone of Åkerberg. The investigation aimed to determine if there also were an oblique kinematic component involved, and in that case determine the relative degree of the oblique movement.

To investigate the block movement, the ChRM-directions obtained from Åke 1 and Åke 2 should be compared to the ChRM-directions of Fåg 1. In Chapter 8.2, however, it was concluded that the directions obtained from monoclinic pyrrhotite of both these outcrops were acquired during the same event and they cannot be separated.

So far, there is no evidence of a magnetite component in Åke 1 and Åke 2, which were found in Fåg 1. The lack of a magnetite component implies that a comparison of a higher stability component cannot be done. On this basis, it is therefore not possible to perform this investigation without further sampling in the area.

8. 4 Lowering of the Magnetic Properties of the Gold Bearing Ore Zone

In this chapter, the magnetic properties of the gold bearing ore zone in Åkerberg will be discussed. There are different ways to asses this question. The first part of the chapter will therefore focus on the magnetic properties of the Åkerberg area. The second part will focus on some petrophysical aspects of the ore zone.

The magnetic map in Figure 18 shows that the Åkerberg gold deposit has lower magnetic field values relative to the surrounding areas (excluding the granodiorite). A way to quantify this anomaly is by Figure 19. The solid, blue, green and red lines in this figure illustrate the susceptibilities, Köningsberger ratios and NRM-intensities of the samples respectively. The dashed lines and the enlargement of site Åke 1 are to illustrate a volume loss due to quartz filled veins, which will be discussed later in this chapter. Comparing outcrop Åke 1 with Åke 2 it is clear that Åke 1 has a two to three orders lower susceptibility compared to Åke 2. (the mean susceptibility value for the outcrops are reported in Table 5). The low susceptibility values and therefore the magnetic anomaly in the shear zone are explained by a relative lower amount of pyrrhotite in theses samples, since susceptibility can be used to assess ferrimagnetic grain concentrations (Peters & Dekkers, 2003).

The amount of pyrrhotite explains the anomaly of the Åkerberg deposit, but not why the amount of pyrrhotite is lower in the ore zone. So far, there is no evidence of varying oxidation states in pyrrhotite, which by chance could affect the bulk susceptibilities of the samples.

An apparent and maybe striking explanation for the magnetic anomaly is a bulk-rock-volume-loss due to abundant quartz veins. To address this question, a short review of the shear zone is necessary. In Chapter 2.2.1, it was reported that millimeter thick quartz veins cut the Åkerberg ore zone. Calculations of exploration drill holes showed that quartz veins constituted between 8-10% of the volume of the rock (pers. comm. Benny Mattson, 2006).This implies that a weakly paramagnetic mineral, e.g. quartz, constitutes 8-10% of the ore zone. As paramagnetic mineral do not contribute to the NRM of a rock, quartz veins would lower the susceptibility of the rock 8-10%. In order to restore the original petrophysical properties of the ore zone (e.g. before mining started), it is assumed that the quartz veins constituted 10 % of the volume in the ore zone. The bulk-rock-volume containing ferrimagnetic minerals would therefore decrease by 10% due to the quartz veins. (It should also be pointed out that the samples from the ore zone did not contain any quartz veins). This decrease lowers the susceptibility, which is shown in Figure 19. The blue dashed line shows the susceptibility after a volume decrease of 10%. The blue solid line represents the susceptibility of the samples in outcrop Åke 1. Comparing these recalculated susceptibilities to outcrop Åke 2, it becomes clear that the interpretation that the amount of pyrrhotite is lower in Åke 1 compared to Åke 2 and Åke 3 remains the same. Quartz veins have therefore not caused the lower susceptibility in the ore zone.

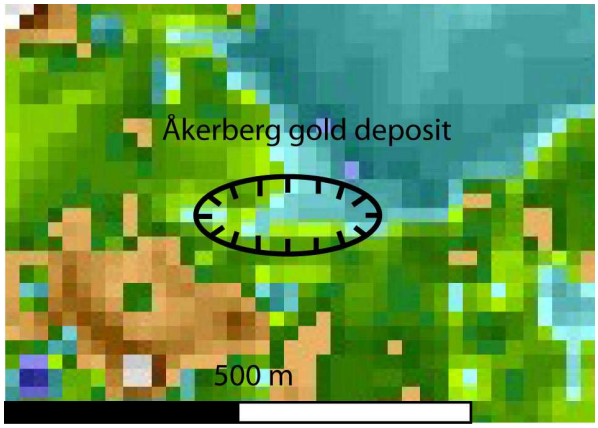

Figure 18. Magnetic anomaly map of the Åkerberg gold deposit. The anomaly is indicated by the color blue in the open cut mine. Modified after a map supplied by Boliden Mineral AB.

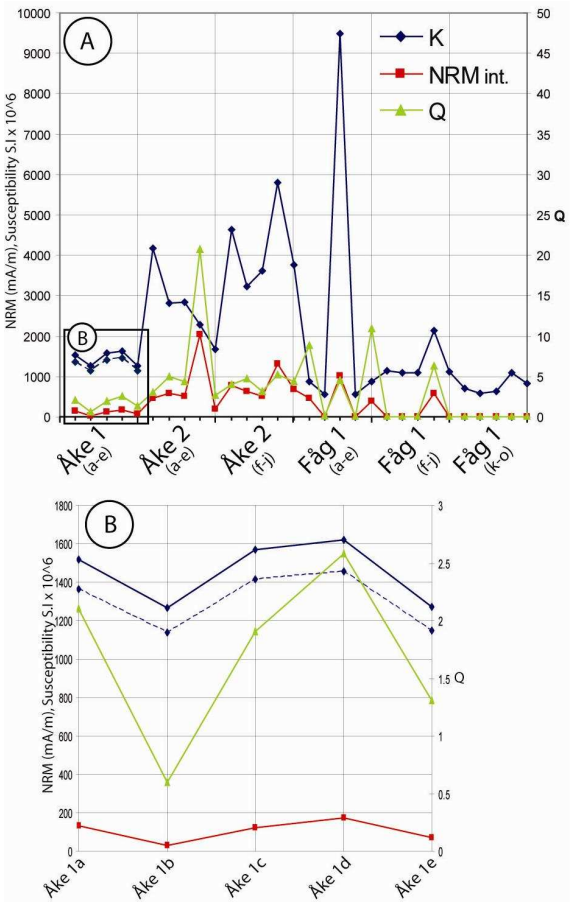

Figure 19. A) Rock magnetic properties of the sampled sites. K= Susceptibility. NRM-int= NRM-intensity. Q= Köningsberger ratios. B) shows the effect on K after a 10% volume loss. The volume loss is due to penetrating quartz veins discussed in the text.

9 Suggestion to Further Studies

Results from the research conducted in this thesis have shown that the amount of monoclinic pyrrhotite is lower in the ore zone compared to the surrounding areas. This lower amount of monoclinic pyrrhotite causes the magnetic anomaly over the area. It is not possible, however, with the results presented in this paper to determine why the amount of monoclinic pyrrhotite is lower in the ore zone. To investigate why the amount of monoclinic pyrrhotite is low, several factors have to be taken into account, such as alteration of magnetic minerals. Guilbert & Park (1986) reports of hydrolysis of wall rock due to hydrothermal fluids. Hydrolysis would lead to an increase of sulfides and a decrease of iron-oxides. Other related work, which addresses alteration of magnetic minerals have been conducted by Airo (2001). Airo (2001) reports of common alteration processes of magnetic minerals, such as magnetite and monoclinic pyrrhotite. According to Airo (2001), magnetite is commonly destroyed in alteration processes such as, biotitization, and sulfidization and silicification, whereas the amount of pyrrhotite is enhanced by reducing hydrothermal fluids. The effects of hydrothermal fluids should therefore be address if the processes that have created the anomaly should be investigated properly. However, the petrological properties of the gabbro may obstruct such investigations. These properties include for example the compositional heterogeneity, which a layered gabbro implies.

This thesis has also yielded interesting results for research concerned with the regional crustal evolution in the area. The analyzed ChRM-directions in this thesis showed that all sampled outcrops had acquired their monoclinic ChRM-directions at the same event. The timing of this event was however, statistically uncertain. But further investigations could address this indicated age (~950 Ma) by assessing the rock magnetic properties in other parts of the meta-gabbro as well as in surrounding rock units. Such investigations should address NRM carried by monoclinic pyrrhotite as the results in this thesis indicate that the magnetite component is older. The investigations should aim to determine several paleomagnetic poles and compared these to previous reported paleomagnetic poles. Such work would show if the indicated age is correct or if it can be dismissed.

10 Conclusions

- Two types of ferrimagnetic minerals carry the NRM in the investigated outcrops. In Åke 1 and Åke 2, monoclinic pyrrhotite. In Fåg 1 monoclinic pyrrhotite is dominating, but there is also evidence of a magnetite component in outcrop Fåg 1.

- The magnetic anomaly of the ore zone is due to a lower amount of monoclinic pyrrhotite relative surrounding areas.

- Monoclinic pyrrhotite has acquired its present NRM during the same event at all sampled localities. The timing of this event, however, is unclear since only one VGP could be calculated.

- Quartz veins cannot explain the magnetic anomaly of the ore zone, as the bulk-rock-volume-loss caused by these joints is too small for the results to be interpreted differently.

11 Acknowledgement

I would like to thank my supervisors Erik Eneroth, Jakob Fahlgren and Benny Mattsson for all the time they spent reviewing various forms of the manuscript and discussing this project with me. I am very grateful to them.

I would also like to acknowledge some people, who have been very helpful during the works progress. Thanks to Tania Stanton and Ian Snowball for instructive assistance in the paleomagnetic laboratory. Thank you to Carl Alwmark and Anders Lindh for help with the SEM-equipment and Daniel Larsson for interesting discussions and showing me reflected light microscopy.

12 References

Airo, M.L., 2001: Aeromagnetic and Aeroradiometric Response to Hydrothermal Alteration. *Surveys in Geophysics,* Vol. **23**, 273-302.

Allen, R., Weihed, P., & Svensson, S-Å., 1997: Set ting of Zn-Cu-Au-Ag massive Sulfide Deposits in the Evolution and Facies Architecture of a 1.9 Ga Marine Volcanic Arc, Skellefte District, Sweden, *Economic Geology*, Vol. **91**, 1022-1053.

Bergman Weihed, J., 1997: Regional deformation zones in the Skellefte and Arvidsjaur areas, *Final research report of SGU-project: 03-862/93,* 35 pp.

Butler, F.R., 1991: *Paleomagnetism*. Blackwell Scientific Publications Ltd, Oxford, 319 pp.

Dekkers, M.J., 1989: Magnetic properties of natural pyrrhotite. II. High- and low-temperature behaveior of J_{rs} and TRM as function of grain size, *Physics of the Earth and Planetary Interiors*, Vol **57**, 266-283.

Deer, W.A., Howie, R.A., & Zussman, J., 1992: *An Introduction to the Rock Forming Minerals*. 2nd edition. Pearson Education Limited, Edinburgh, 696 pp.

Dunlop, D., & Özdemir, Ö., 2001: *Rock Magnetism Fundamentals and Frontiers*. Paper back edition, Cambridge University Press, Cambridge, 573 pp.

Geodynamics, September, 2006: www.geodynamics.no.

Guilbert, J., Park, C., 1986: *The Geology of Ore Deposits*. W.H. Freeman and Company, New York, 985 pp.

Hunt, P., Moskowitz, C., Bruce, M., & Banerjee, K.S., 1995: Magnetic Properties of Rocks and Minerals. In: Ahrens T.J ed: *Rock physics and phase Relations*, A Handbook of Physical Constants, American Physical Union, 189-204 pp.

Kathol, B., & Weihed, P., 2005: *Description of re gional geological and geophysical maps of the Skellefte District and surrounding areas*. Sveriges Geologiska Undersökning, Uppsala, 197 pp. ISBN: 91-7158-678-4.

Kjöde, J., 1980: Paleomagnetism of the late Precam brian dolerite dykes from Varanger peninsula, north Norway. *Physics of the Earth and Planetary Interiors*, Vol. **21**(1), 38-49.

Lindström, M., Lundqvist, J., & Lundqvist, T., 2000: *Sveriges geologi från urtid till nutid*. 2nd edition. Studentlitteratur, Lund, 491 pp.

Lundström, I., & Antal, I., 2000: Bergrundskartan 23K Boliden SO, Sveriges Geologiska Undersök ning.

Mattson, B., 1991: *Mineralmarknaden Tema: Krom*. Sveriges Geologiska Undersökning, Uppsala, 32-34 pp.

Meert, J.G., Torsvik., T.H, Eide, E.A., & Dahlgren, S., 1998: Tectonic significance of the Fen Prov ince, S. Norway: Constraints from geochronology and Paleomagnetism. *Journal of Geology*, Vol. **106**(5), 553-564.

Mertanen, S., Pesonen, L.J., & Huhma, H., 1996: Paleomagnetism and Sm-Nd ages of the Neopro terozoic diabase dykes in Laanila and Kautokeino, northern Fennoscandia. *Precambrian crustal evolution in the North Atlantic region – Geological society London*; *Special publication*, Vol. **112**, 331-358.

National Geophysical Data Centre., November 2006: www.ngdc.noaa.gov.

Neuvonen, J.K., 1966: Paleomagnetism of the dike system in Finland; II, Remanent magnetization of dolerites in the Vaasa archipelago. *Bulletin de la Commission Geologique de Finlande*, Vol. **222**; 38, 275-281.

Patchett, P.J & Bylund, G., 1977: Age of Grenville Belt magnetisation: Rb-Sr and paleomagnetic evidence from Swedish dolerites. *Earth and Planetary Science Letters,* Vol. **35**(1), 92-104.

Piper, J.D.A., 1981. Magnetic properties of the Alnö Complex, Sweden. *Geologiska Föreningens i Stockholms Förhandlingar*, Vol. **103**(1), 9-15.

Pesonen, L.J., Bylund, G., Torsvik, T.H., Elming, S.Å., & Mertanen, S., 1991: Catalogue of palaeomagnetic directions and poles from the Fennoscandia: Archaean to Tertiary. *Tectonphysics*, Vol. **195**, 151-207.

Peters, C., & Dekkers, M.J., 2003: Selected room temperature magnetic parameters as a function of mineralogy, concentraion and grain size. *Physics and Chemistry of the Earth*, Vol. **28**, 659-667.

Sundblad, K., 2003.Metallogeny of gold in the Pre cambrian of Northern Europe. *Economic Geol ogy*, Vol. **98**, 1271-1290.

Torsvik, T.H., Robert, D., & Siedlecka, A., 1995: Paleomagnetic data from sedimentary rocks and dolerite dykes, Kildin Island, Rybachi, Serdni and Varanger peninsulas, NW Russia and NE Norway; a review. *Special publication Norges Geol giske Undersokelse*, Vol. **7**, 315-326.

Torsvik, T.H., & Rehnström, E.F., 2001: Cambrian paleomagnetic data from Baltica: Implications for true polar wonder and Cambrian paleogeography. *Journal of the Geological Society*, Vol. **158**(2), 321-330.

Weihed, P, 1992: Litogeochmistry, metal and altera tion zoning in the Proterozic Tallberg porphyry-type deposit, northern Sweden, *Journal of geochemical exploration*, Vol. **42**, 301-325.

Weihed, P., Ardnt, N., Billström, K., Dunchesne, J-C., Eilu, P., Martinsson, O., Papunen, H., & Lahtinen, R., 2005: Precambrian geodynamics and ore formation: The Fennoscandian Shield. *Ore Geology Reviews*, Vol. **27**, 273-322.

Welin, E, 1987: The Depositional Evolution of the Svecofennian Supracrustal Sequence in Finland and Sweden, *Precambrian Research*, Vol. **35**, 95-113.

Appendix 1

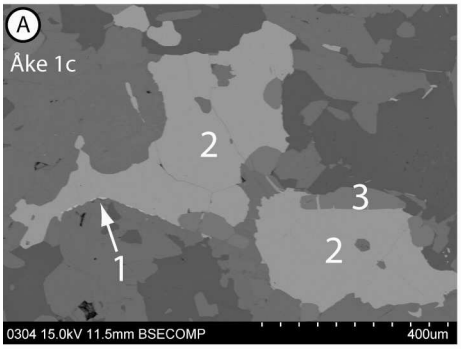

Figure A. SEM-photo of: 1) Zircon. 2) Ilmenite. 3) Apatite. Corresponding SEM-spectrum for each mineral is shown to the right.

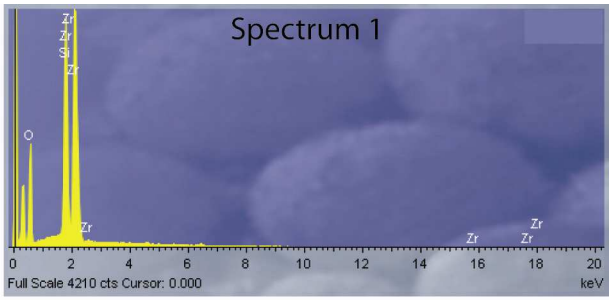

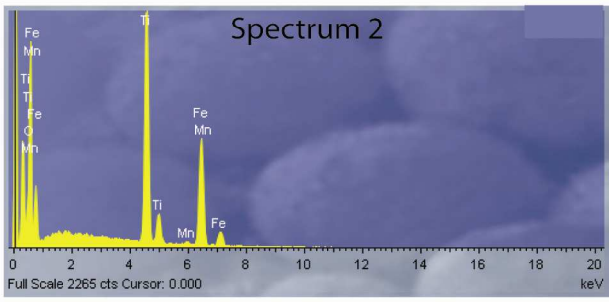

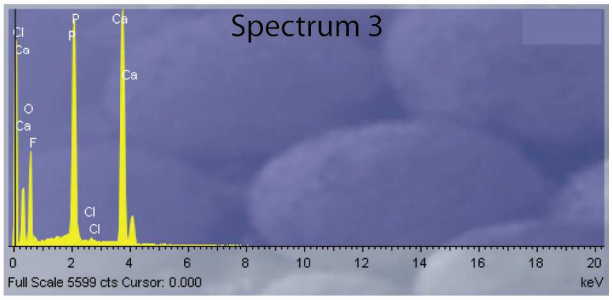

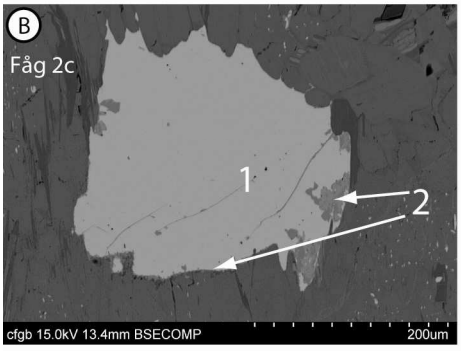

Figure B. SEM-photo of: 1) Ilmenite. 2) Rutile. Corresponding SEM-spectrum for each mineral is shown to the right.

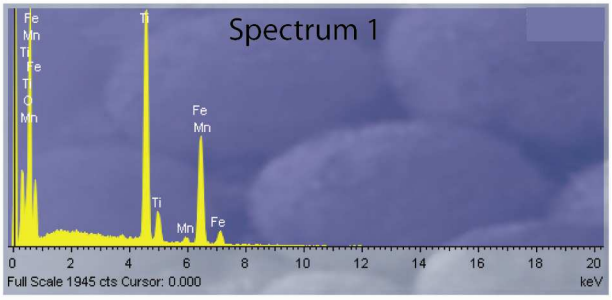

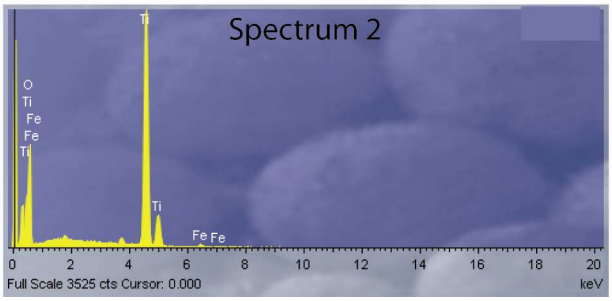

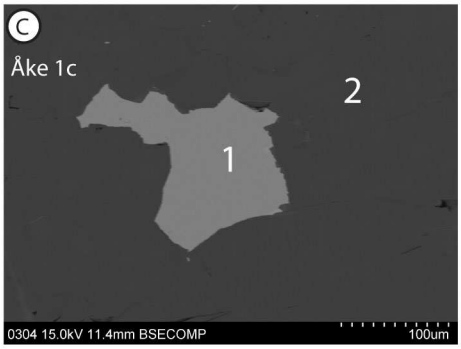

Figure C. SEM-photo of: 1) Pyrrhotite. 2) Amphibole. Corresponding SEM-spectrum for each mineral is shown to the right.

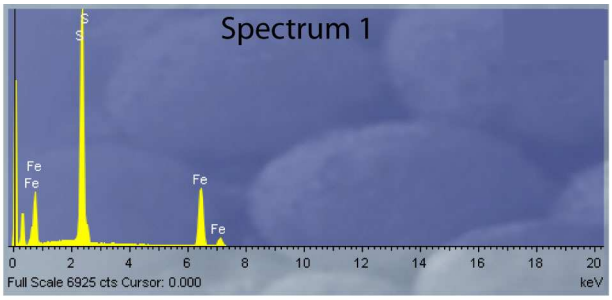

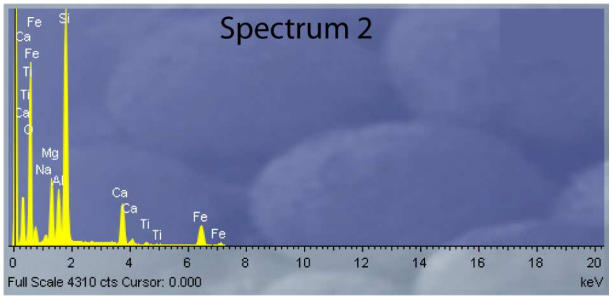

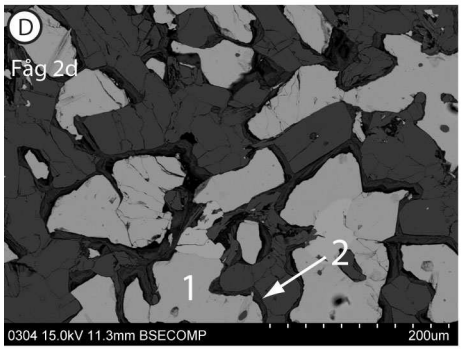

Figure D. SEM-photo of: 1) Pyrrhotite. 2) Chlorite corona. Corresponding SEM-spectrum for each mineral is shown to the right.

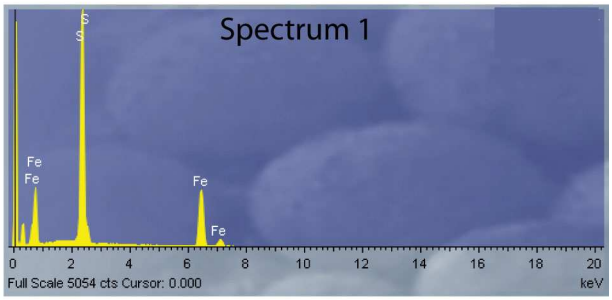

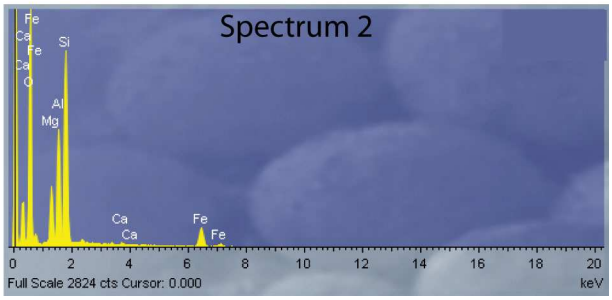

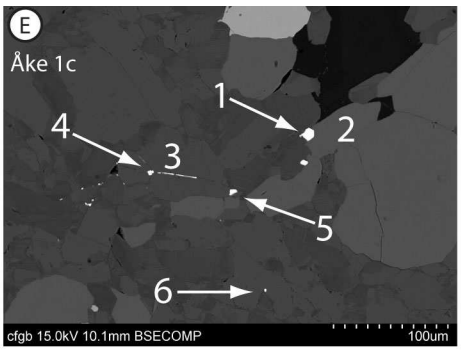

Figure 1. SEM-photo of: 1) Gold. 2) Apatite. 3) Pyroxene. 4) Gold 5) Sphalerite. 6) Scheelite. Corresponding SEM-spectrum for each mineral is shown to the right.

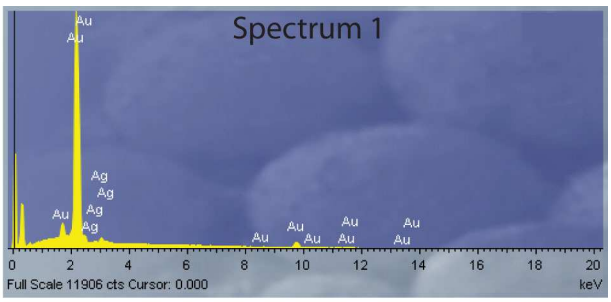

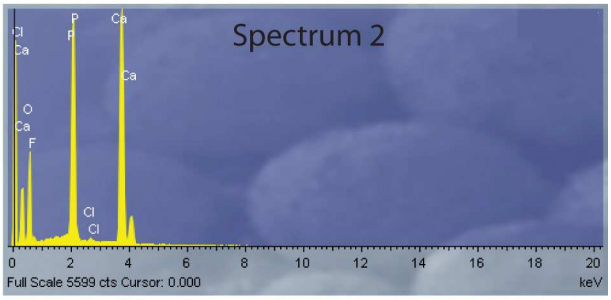

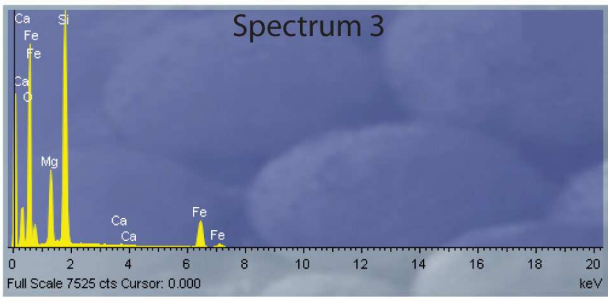

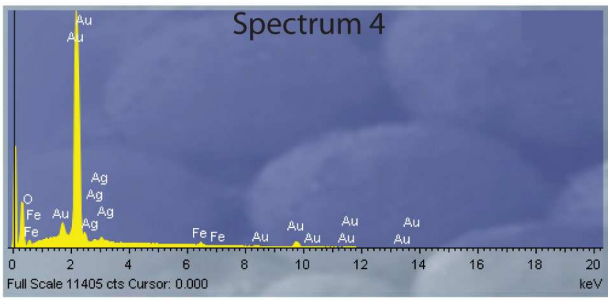

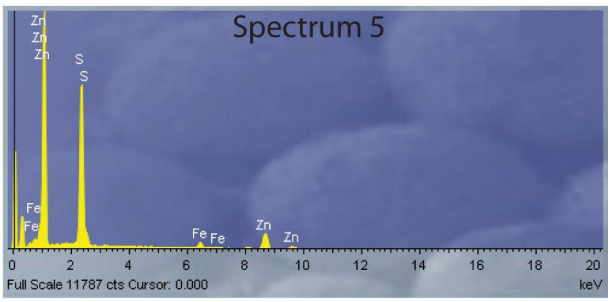

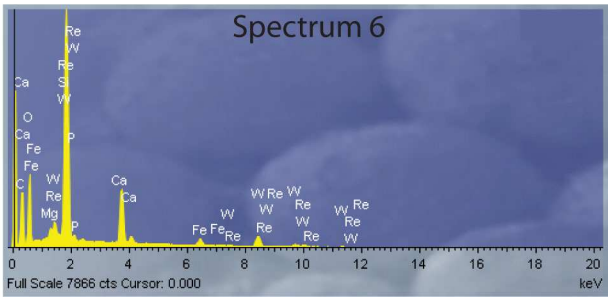

Tidigare skrifter i serien "Examensarbeten i Geologi vid Lunds Universitet":

160. Fuchs, M., 2003: Påverkan av sterilisering på gruvsand – en mineralogisk och texturell undersökning.
161. Ljungberg, Julia, 2003. Sierggavággeskollan i gränslandet mellan Sarek och Padjelanta; miljöindikatorer för fjällkedjeberggrundens bildning.
162. Håkansson, Lena, 2003: An architectural element analysis of a large-scale thrust complex, Kanin Peninsula, NW Russia: interaction between the Barents and Kara Sea ice sheets.
163. Davidson, Anja, 2003: Ignimbritenheterna i Barranco de Tiritaña, övre Mogánformationen, Gran Canaria.
164. Näsström, Helena, 2003: Klotdioriten vid Slättemossa, centrala Småland – mineralkemi och genes.
165. Nilsson, Andreas, 2003: Early Ludlow (Silurian) graptolites from Skåne, southern Sweden.
166. Dou, Marion, 2003: Les ferromagnésiens du granite rapakivique de Nordingrå – centre-est de la Suède – composition chimique et stade final de cristallisation.
167. Jönsson, Emma, 2003: En pollenanalytisk studie av råhumusprofiler från Säröhalvön i norra Halland.
168. Alwmark, Carl, 2003: Magmatisk och metamorf petrologi av en mafisk intrusion i Mylonitzonen.
169. Pettersson, Ann, 2003: Jämförande litologisk och geokemisk studie av Sevens amfibolitkomplex i Sylarna och Kebnekaise.
170. Axelsson, Katarina, 2004: Bedömning av potentiell föroreningsspridning från ett avfallsupplag utanför Löddeköpinge, Skåne.
171. Ekestubbe, Jonas, 2004: $^{40}Ar/^{39}Ar$ geokronologi och implikationer för tolkningen av den Kaledoniska utvecklingen i Kebnekaise.
172. Lindgren, Paula, 2004. Tre sensvekofenniska graniter: kontakt- och åldersrelationer samt förekomst av metasedimentära enklaver.
173. Janson, Charlotta, 2004. A petrographical and geochemical study of granitoids from the south-eastern part of the Linderödsåsen Horst, Skåne.
174. Jonsson, Sara, 2004: Structural control of fine-grained granite dykes at the Äspö Hard Rock Laboratory, north of Oskarshamn, Sweden.
175. Ljungberg, Carina, 2004: Belemniters stabila isotopsammansättning: paleomiljöns och diagenesens betydelse.
176. Oster, Jessica, 2004: A stratigraphic study of a coastal section through a Late Weichselian kettle hole basin at Ålabodarna, western Skåne, Sweden.
177. Einarsson, Elisabeth, 2004: Morphological and functional differences between rhamphorhynchoid and pterodactyloid pterosaurs with emphasis on flight.
178. Anell, Ingrid, 2004: Subsidence in rift zones; Analyzing results from repeated precision leveling of the Vogar Profile on the Reykjanes Peninsula, Southwest Iceland.
179. Wall, Torbjörn, 2004: Magnetic grain-size analyses of Holocene sediments in the North Atlantic and Norwegian Sea – palaeoceano-graphic applications.
180. Mellgren, Johanna, S., 2005: A model of reconstruction for the oral apparatus of the Ordovician conodont genus *Protopanderodus* Lindström, 1971.
181. Jansson, Cecilia, 2005: Krossbergskvalitet och petrografi i den kambriska Hardebergasandstenen i Skåne.
182. Öst, Jan-Olof, 2005: En övergripande beskrivning av malmbildande processer med detaljstudier av en bandad järnmalm från södra Dalarna, Bergslagen.
183. Bragée, Petra, 2005: A palaeoecological study of Holocene lake sediments above the highest shoreline in the province of Västerbotten, northeast Sweden.
184. Larsson, Peter, 2005: Palynofacies och mineralogi över krita-paleogengränsen vid Stevns Klint och Kjølby Gaard, Danmark.
185. Åberg, Lina, 2005: Metamorphic study of metasediment from the Kangilinaaq Peninsula, West Greenland.
186. Sidgren, Ann-Sofie, 2005: $^{40}Ar/^{39}Ar$-geokronologi i det Rinkiska bältet, västra Grönland.
187. Gustavsson, Lena, 2005: The Late Silurian Lau Event and brachiopods from Gotland, Sweden.

188. Nilsson, Eva K., 2005: Extinctions and faunal turnovers of early vertebrates during the Late Silurian Lau Event, Gotland, Sweden.
189. Czarniecka, Ursula, 2005: Investigations of infiltration basins at the Vomb Water Plant – a study of possible causes of reduced infiltration capacity.
190. G³owacka, Ma³gorzata, 2005: Soil and groundwater contamination with gasoline and diesel oil. Assessment of subsurface hydrocarbon contamination resulting from a fuel release from an underground storage tank in Vanstad, Skåne, Sweden.
191. Wennerberg, Hans, 2005: A study of early Holocene climate changes in Småland, Sweden, with focus on the '8.2 kyr event'.
192. Nolvi, Maria & Thorelli, Gunilla, 2006: Extraterrestrisk och terrestrisk kromrik spinell i fanerozoiska kondenserade sediment.
193. Nilsson, Andreas, 2006: Palaeomagnetic secular variations in the varved sediments of Lake Goœci¹¿, Poland: testing the stability of the natural remanent magnetization and validity of relative palaeointensity estimates.
194. Nilsson, Anders, 2006: Limnological responses to late Holocene permafrost dynamics at the Stordalen mire, Abisko, northern Sweden.
195. Nilsson, Susanne, 2006: Sedimentary facies and fauna of the Late Silurian Bjärsjölagård Limestone Member (Klinta Formation), Skåne, Sweden.
196. Sköld, Eva, 2006: Kulturlandskapets förändringar inom röjningsröseområdet Yttra Berg, Halland - en pollenanalytisk undersökning av de senaste 5000 åren.
197. Göransson, Ammy, 2006: Lokala miljöförändringar i samband med en plötslig havsyteförändring ca 8200 år före nutid vid Kalvöviken i centrala Blekinge.
198. Brunzell, Anna, 2006: Geofysiska mätningar och visualisering för bedömning av heterogeniteters utbredning i en isälvsavlagring med betydelse för grundvattenflöde.
199. Erlfeldt, Åsa, 2006: Brachiopod faunal dynamics during the Silurian Ireviken Event, Gotland, Sweden.
200. Vollert, Victoria, 2006: Petrografisk och geokemisk karaktärisering av metabasiter i Herrestadsområdet, Småland.
201. Rasmussen, Karin, 2006: En provenansstudie av Kågerödformationen i NV Skåne – tungmineral och petrografi.
202. Karlsson, Jonnina, P., 2006: An investigation of the Felsic Ramiane Pluton, in the Monapo Structure, Northern Moçambique.
203. Jansson, Ida-Maria, 2006: An Early Jurassic conifer-dominated assemblage of the Clarence-Moreton Basin, eastern Australia.
204. Striberger, Johan, 2006: En lito- och biostratigrafisk studie av senglaciala sediment från Skuremåla, Blekinge.
205. Bergelin, Ingemar, 2006: $^{40}Ar/^{39}Ar$ geochronology of basalts in Scania, S Sweden: evidence for two pulses at 191-178 Ma and 110 Ma, and their relation to the breakup of Pangea.
206. Edvarssson, Johannes, 2006: Dendrokronologisk undersökning av tallbestånds etablering, tillväxtdynamik och degenerering orsakat av klimatrelaterade hydrologiska variationer på Viss mosse och Åbuamossen, Skåne, södra Sverige, 7300-3200 cal. BP.
207. Stenfeldt, Fredrik, 2006: Litostratigrafiska studier av en platåformad sand- och grusavlagring i Skuremåla, Blekinge.
208. Dahlenborg, Lars, 2007: A Rock Magnetic Study of the Åkerberg Gold Deposit, Northern Sweden.
209. Olsson, Johan, 2007: Två svekofenniska graniter i Bottniska bassängen; utbredning, U-Pb zirkondatering och test av olika abrasionstekniker.

LUNDS UNIVERSITET

Geologiska institutionen
Gentrum för GeoBiosfärsvetenskap
Sölvegatan 12, 223 62 Lund